

1 **Title:** Does phenology explain plant-pollinator interactions at different latitudes? An assessment of its
2 explanatory power in plant-hoverfly networks in French calcareous grasslands

3 **Authors:** Natasha de Manincor^{1*}, Nina Hautekeete¹, Yves Piquot¹, Bertrand Schatz², Cédric
4 Vanappelghem³, François Massol^{1,4}

5 ¹Université de Lille, CNRS, UMR 8198 - Evo-Eco-Paleo, F-59000 Lille, France

6 ²CEFE, EPHE-PSL, CNRS, University of Montpellier, University of Paul Valéry Montpellier 3, IRD,
7 Montpellier, France

8 ³Conservatoire d'espaces naturels Nord et du Pas-de-Calais, 160 rue Achille Fanien - ZA de la Haye,
9 62190 LILLERS

10 ⁴Univ. Lille, CNRS, Inserm, CHU Lille, Institut Pasteur de Lille, U1019 - UMR 8204 - CIIL - Center for
11 Infection and Immunity of Lille, F-59000 Lille, France

12

13 E-mail addresses and ORCID numbers:

14 Natasha de Manincor: natasha.de-manincor@univ-lille.fr, 0000-0001-9696-125X

15 Nina Hautekeete: nina.hautekeete@univ-lille.fr, 0000-0002-6071-5601

16 Yves Piquot: yves.piquot@univ-lille.fr, 0000-0001-9977-8936

17 Bertrand Schatz: bertrand.schatz@cefe.cnrs.fr, 0000-0003-0135-8154

18 Cédric Vanappelghem: cedric.vanappelghem@espaces-naturels.fr

19 François Massol: francois.massol@univ-lille.fr, 0000-0002-4098-955X

20

21 **Short title:** Phenology and plant-hoverfly interactions

22 **Keywords:** Bayesian model, interaction probability, latent block model, latitudinal gradient,
23 mutualistic network, phenology overlap, species abundance, structural equation model.

24 *Corresponding author information: Natasha de Manincor, e-mail: natasha.de-manincor@univ-lille.fr,

25 phone: +330362268530

26 **Author contributions**

27 NDM and FM conceived the project, formulated and implemented the model. NDM conducted the
28 analysis and prepared the manuscript. FM supervised the analysis and edited the manuscript. NH, YP,
29 CV and BS contributed substantially to all later versions. NDM, NH, YP and BS conducted the fieldwork
30 and provided the data. CV identified the hoverflies.

31 **Data accessibility**

32 The data supporting the results are archived on Zenodo (DOI: [10.5281/zenodo.2542845](https://doi.org/10.5281/zenodo.2542845)).

33

34 **Abstract**

35 For plant-pollinator interactions to occur, the flowering of plants and the flying period of pollinators
36 (*i.e.* their phenologies) have to overlap. Yet, few models make use of this principle to predict
37 interactions and fewer still are able to compare interaction networks of different sizes. Here, we
38 tackled both challenges using Bayesian Structural Equation Models (SEM), incorporating the effect of
39 phenology overlap, in six plant-hoverfly networks. Insect and plant abundances were strong
40 determinants of the number of visits, while phenology overlap alone was not sufficient, but
41 significantly improved model fit. Phenology overlap was a stronger determinant of plant-pollinator
42 interactions in sites where the average overlap was longer and network compartmentalization was
43 weaker, *i.e.* at higher latitudes. Our approach highlights the advantages of using Bayesian SEMs to
44 compare interaction networks of different sizes along environmental gradients and articulates the
45 various steps needed to do so.

46

Supprimé :

48 **INTRODUCTION**

49 Understanding how phenology determines species interactions is a central question in the case of
50 mutualistic networks. In plant-pollinator networks, phenology shapes their temporal and spatial limits,
51 thus defining the area and the period along the season in which interactions preferably occur (Olesen
52 *et al.* 2011; Ogilvie & Forrest 2017). Since plant and pollinator phenologies are not equally affected by
53 changes in environmental cues, partial or total phenological mismatches can occur as a result of
54 environmental changes such as climate change (Parmesan 2007; Rafferty 2017). Phenological
55 advances indeed increase at higher latitudes, as a response to the acceleration of warming
56 temperature along the same gradient (Post *et al.* 2018), increase phenological mismatch, and have the
57 potential to threaten the synchrony needed for effective pollination (Hutchings *et al.* 2018). Such
58 environmental changes can thus drastically alter pollinator interactions through modified temporal
59 overlap between pollinators and their floral resources leading, in extreme cases, to local extinctions
60 (Memmott *et al.* 2007) and the ensuing absence of the partner species at the location and/or time at
61 which the interaction should have taken place (Willmer 2012; Miller-Struttman *et al.* 2015; Rafferty
62 *et al.* 2015; Hutchings *et al.* 2018).

63 Because phenological match is crucial to plant-pollinator interactions, and thus ultimately to
64 pollinators' fitness, pollinators have to adapt to phenological shifts either through interaction with
65 other plant species (Rafferty *et al.* 2015) or through changes of their own phenology (Bartomeus *et al.*
66 2011). Phenology can then influence dynamical network properties, such as the stability and the
67 coexistence of species, through changes in network topology (Encinas-Viso *et al.* 2012). Moreover,
68 phenology predictably affects network compartmentalization as different phenophases likely
69 correspond to different compartments when networks are considered on an annual scale (Martín
70 González *et al.* 2012).

71 Despite considerable theoretical advances, there are few models available to predict the probability
72 of interaction in plant-pollinator networks (Staniczenko *et al.* 2017; Cirtwill *et al.* 2019) and fewer still

73 able to make comparisons between networks. Due to their complexity and variation among years
74 (Chacoff *et al.* 2017), most studies of mutualistic networks have focused on predicting and comparing
75 classic network metrics (nestedness, connectance, modularity, etc.) which are all influenced by
76 network size, *i.e.* the number of plant and insect species (Fortuna *et al.* 2010; Staniczenko *et al.* 2013;
77 Poisot & Gravel 2014; Astegiano *et al.* 2015). Moreover, few studies have compared interaction
78 networks along environmental gradients (Devoto *et al.* 2005; Schleuning *et al.* 2012; Sebastián-
79 González *et al.* 2015; Pellissier *et al.* 2017). In order to compare networks of different sizes, a better
80 alternative is to switch from network-derived metrics to the comparison of the probability of
81 interaction given by regression models, which can consider multiple factors and latent variables and
82 assume that the sampled data are just part of a larger unobserved dataset (Grace *et al.* 2010).
83 Calcareous grasslands are characterized by highly diverse plant communities with a high proportion of
84 entomophilous species (Baude *et al.* 2016), thus they are a convenient model for such studies. Most
85 plant-insect pollinator networks involve bee species (Anthophila), but recent studies have also pointed
86 out the importance of hoverflies (Diptera: Syrphidae), which pollinate a large spectrum of wild
87 flowering species (Klecka *et al.* 2018a) and crops (Jauker & Wolters 2008; Rader *et al.* 2011). They
88 usually behave opportunistically, *i.e.* from being pollen generalists to specialists, only limited by
89 morphological constraints (Iler *et al.* 2013; Klecka *et al.* 2018a; Lucas *et al.* 2018). Indeed, their
90 generalist behaviour, at the species level, could be the result of individually specialized diets, since
91 most pollen retrieved on hoverfly individuals usually comes from a single plant taxon (Lucas *et al.* 2018)
92 and depends on flower availability and phenology (Cowgill *et al.* 1993; Colley & Luna 2000; Lucas *et al.*
93 2018). Moreover, some hoverflies have preferences regarding plant colour, morphology and
94 inflorescence height (Branquart & Hemptinne 2000; Colley & Luna 2000; Lunau 2014; Klecka *et al.*
95 2018b, a).

96 Here we study the consequences of environmental gradients on plant-pollinator interactions, focusing
97 on how phenology overlap affects interactions between plants and insects in six calcareous grassland

Mis en forme : Anglais (Royaume-Uni)

Mis en forme : Anglais (Royaume-Uni)

Supprimé: output

Supprimé: Large datasets allowing relevant comparisons of networks are rare; they require parallel investigations in rich communities of plants and insects to favour interactions between them. ¶

Supprimé: as well as pollen or nectar

Supprimé: ation

Supprimé: serial

106 sites distributed along a latitudinal gradient. We obtained plant and insect phenologies, abundances,
107 and interactions in all sites from April to October 2016. We modelled plant-pollinator interaction
108 networks following a Bayesian Structural Equation Modelling approach (SEM) using latent variables,
109 [i.e. unobserved variables](#) (Grace *et al.* 2010). [SEM is a multivariate technique used to test several](#)
110 [hypotheses in ecological studies. SEM analysis involves cause-effect equations to evaluate multiple](#)
111 [causal relationship](#) (Grace 2006; Eisenhauer *et al.* 2015) [using observed and latent variables to explain](#)
112 [some other observed variables](#) (Grace 2006). [SEM can be used to choose among competing models](#)
113 (Grace & Bollen 2008). [Thus, SEM are well suited for studying the complexity of ecological networks.](#)
114 [To test whether phenology affects network compartmentalization, we looked for species subgroups](#)
115 [using a latent block model \(LBM\) which is among the best clustering methods for weighted networks](#)
116 (Leger *et al.* 2015).

117 The comparison of 16 SEMs and the analysis of LBMs of sampled networks evinced that phenology
118 overlap is an important determinant of plant-pollinator interactions, but is less informative than
119 species abundances and performs heterogeneously among sites. Our results suggest that the use of
120 SEMs to compare networks of different sizes along an environmental gradient is an innovative
121 approach which can help understand the structure of plant-pollinator networks.

122 MATERIALS AND METHODS

123 Study sites

124 We sampled plant and [hoverfly](#) species in six areas (Fig. S1) of 1 hectare each in different French
125 regions: two sites in Hauts-de-France (Les Larris de Grouches-Luchuel, thereafter noted LAR,
126 50°11'22.5"N 2°22'02.9"E and Regional natural reserve Riez de Noeux les Auxi, noted R, 50°14'51.85"N
127 2°12'05.56"E, in départements Pas-de-Calais and Somme), two sites in Normandie (Château Gaillard –
128 le Bois Dumont, noted CG, 49°14'7.782"N 1°24'16.445"E and les Falaises d'Orival, noted FAL,
129 49°04'40.08"N 1°33'07.254"E, départements: Eure and Seine Maritime) and two sites in Occitanie
130 (Fourches, noted F, 43°56'07.00"N 3°30'46.1"E and Bois de Fontaret, noted BF, 43°55'17.71"N

Supprimé: pollinator

132 3°30'06.06"E, département: Gard). The six sites are included in the European NATURA 2000 network, [a](#)
133 [network of preserved areas designated to protect a number of habitats and species representative of](#)
134 [European biodiversity](#). The four sites in Hauts-de-France and Normandie are managed by the
135 Conservatoire d'espaces naturels of Normandie, Picardie and Nord – Pas-de-Calais and the sites in
136 Occitanie by the CPIE Causses méridionaux. We sampled each site once a month from April to October
137 2016, except for the site of Riez that was sampled from May to October.

138 Plant-hoverfly observations and sampling

139 To collect information at the community level, in each site and at each session we realized: (i) a botanic
140 inventory of the flowering species, recorded their abundances and the total flower covering in the area
141 and (ii) a pollinator sampling using a hand net along a variable transect walk.

142 Flowering plants were identified at the species level. We recorded the abundances of all flowering
143 species. At first, we estimated the total percentage of surface covered by all flowering species in the
144 selected area. We then estimated the relative abundance of each flowering species. We used Braun-
145 Blanquet coefficients of abundance-dominance, [ranked from i to 5 \(most abundant coefficient class\)](#)
146 (Van Der Maarel 1975, 1979; Mucina *et al.* 2000), to rank flowering species. [We converted the](#)
147 [coefficients to percentage intervals and then in mean values of percentage cover classes \(Table S1\):](#)
148 coefficient **5** = 75-100%, coeff **4** = 50-75%, coeff **3**=25-50%, coeff **2** = 10-25%, coeff **1** = 1-10%, coeff **+**
149 = few individuals less than < 1%, coeff **i** = 1 individual. All inventories were realized by the same
150 surveyors to avoid biases.

151 Pollinator observations were performed by the same team of 3-5 persons each day. The surveyors
152 walked slowly around any potential attractive resource patch included in the selected 1-hectare area
153 for 4h each day. We split the sampling period into 2 hours in the morning (about 10-12h) and 2 hours
154 in the afternoon (about 14-16h) to cover the daily variability of both pollinator (bees and hoverflies,
155 which are more active in the morning than in the afternoon; D'Amen *et al.* 2013) and flower
156 communities. Sampling took place when we had suitable weather conditions for pollinators (following

157 Westphal *et al.* 2008). We sampled all flower-visiting insects and we recorded observed interactions.
158 All sampled insects were immediately put individually in a killing vial with ethyl acetate and were later
159 prepared and pinned in the laboratory and identified at the species level by expert taxonomists. Even
160 if we collected both bees and hoverflies, in this study we focus on [hoverflies](#) only ([since at the moment](#)
161 [of the study bees were not identified at the species level yet](#)). Overall, we sampled for 41 days,
162 equivalent to about 164 hours in the field (all the surveyors collected at the same time). For all analyses
163 described here, we only used the list of visited herbaceous plant species and hoverflies which were
164 found visiting a plant. Despite their rarity [and even if hoverflies are known to prefer open flowers](#)
165 [\(Branquart & Hemptinne 2000\)](#), we also considered the interactions between hoverflies and plant
166 species of the Fabaceae family because [we observed in the field that they visited Fabaceae species](#)
167 [that were already opened by other insects, e.g. by large bee species, such as *Eucera* sp. \(de Manincor,](#)
168 [personal observation\)](#).

Supprimé: we did not want to exclude data in the absence of the proof of no interaction, even if hoverflies are known to prefer open flowers (Branquart & Hemptinne 2000). However,

Supprimé: D

169 Plant – hoverfly networks

170 For each site, we constructed an interaction network consisting of all pairs of interacting plant and
171 insect species, pooling data from all months. A pair of species (i, j) was connected with intensity v_{ij} when
172 we recorded v_{ij} visits of insect species i on plant species j in the site. We calculated the network
173 specialization index, H_2' (Blüthgen *et al.* 2006) using the `H2fun` function implemented in the
174 `bipartite` package (Dormann *et al.* 2009; R Core Team 2018). [We obtained the \$d\$ -value \(Kullback-](#)
175 [Leibler divergence between the interactions of the focal species and the interactions predicted by the](#)
176 [weight of potential partner species in the overall network\) and the \$d_{max}\$ -value \(maximum \$d\$ -value](#)
177 [theoretically possible given the observed number of interactions in the network\) using the `dFUN`](#)
178 [function in the `bipartite` package \(Dormann *et al.* 2009\). \[We did not use the \\$d'\\$ values provided by\]\(#\)
179 \[this package as they sometimes yielded spurious results based on the computation of the minimal \\$d\\$\]\(#\)
180 \[value \\(e.g. reporting low \\$d'\\$ for species with only one partner in the network\\). We \\[then manually\\]\\(#\\)\]\(#\)](#)

Déplacé (insertion) [3]

Supprimé: se values

Supprimé: , but we

Supprimé: ¶

Supprimé: also

190 calculated the standardized specialization index d' (Blüthgen *et al.* 2006) for each plant and insect
191 species as the ratio of the d -value to its corresponding d_{max} -value.
192 We calculated the modularity of the network and the associated partition of species into modules
193 using the `cluster_leading_eigen` method for modularity optimization implemented in the
194 `igraph` package (Csardi & Nepusz 2006; Newman 2006). [Modularity optimization can help identify](#)
195 [strong, simple divisions of a network into relatively independent sub-networks by looking for highly](#)
196 [interconnected sub-networks](#). However, modules are not meant to inform about more subtle
197 groupings among the species, *e.g.* particular avoidance of interactions between insects of group A and
198 plants of group 1. In order to detect such groups, we implemented latent block models (LBM) using
199 the `BM_poisson` method for Poisson probability distribution implemented in the `blockmodels`
200 package (Leger *et al.* 2015). Blocks are calculated separately for the two groups (insect and plant) based
201 on the number of visits (*i.e.* a weighted network). The algorithm finds the best divisions of insects and
202 plants through fitting one Poisson parameter in each block of the visit matrix, thus essentially
203 maximizing the ICL (Integrated Completed Likelihood; Biernacki *et al.* 2000; Daudin *et al.* 2008). The
204 LBM script is given in Supplementary Information (Appendix S3). All analyses were performed in R
205 version 3.3.3 (R Core Team 2018).

206 Plant and hoverfly abundances and phenology overlap

207 We calculated plant abundance using information about the abundance-dominance recorded in the
208 field following the methodology of Braun-Blanquet presented above. We transformed the coefficients
209 of abundance in percentages (Table S1): we used the mean of the percentage corresponding to each
210 class. We then calculated the relative abundance (A_p) of each flowering plant species as the ratio of
211 the focal species cumulated abundance to total flower abundance during its flowering season. [For](#)
212 [hoverflies, we](#) used the recorded number of visiting [individuals \(total abundance\)](#) and their presence
213 (recorded months) along the season to calculate their average abundance during months when they
214 were present (A_H).

Supprimé: (Kullback-Leibler divergence between the interactions of the focal species and the interactions predicted by the weight of potential partner species in the overall network)

Supprimé: (maximum d -value theoretically possible given the observed number of interactions in the network)

Déplacé vers le haut [3]: We obtained these values using the `dFUN` function in the `bipartite` package (Dormann *et al.* 2009), but we did not use the d' values provided by this package as they sometimes yielded spurious results based on the computation of the minimal d value (*e.g.* reporting low d' for species with only one partner in the network).

Supprimé: w

Supprimé: hoverflies

229 We refer to plant phenology as their flowering period and insect phenology as the flying period. We
230 considered only flowering plants which had been visited by pollinators. For the pollinators, we
231 considered only hoverflies which were found in interaction. To build the species phenology tables for
232 both plants and hoverflies, we merged the information provided by two sources of data (field data and
233 the literature): we used the observed phenology of both plants and insects during the field session as
234 the only source of information for plants (plants visited by insects and plants found in the botanic
235 inventory in the site at that date), and we complemented the hoverfly phenology with information
236 provided by the Syrph the Net Database (Speight *et al.* 2016). We then built the phenology overlap
237 (PO) matrix based on the species phenology tables by calculating the number of phenologically active
238 months that are shared by each pair of insect and plant species along the season.

239 Bayesian Structural Equation Modelling (SEM)

240 [SEM is a confirmatory technique that involves cause-effect equations to evaluate multivariate](#)
241 [hypotheses in ecological networks \(Grace 2006\). The primary interest of SEM analyses lies in its ability](#)
242 [to compare different causal models between the same sets of explanatory and explained variables.](#)
243 [Another important feature of SEM is that they can relate data through latent variables, i.e. variables](#)
244 [which are not measured in the model and which represent underlying causes or effects, coupled with](#)
245 [observed variables \(Grace 2006; Grace et al. 2010\). SEM can now be assessed using Bayesian](#)
246 [approaches and parameters estimated using MCMC \(Markov Chain Monte Carlo\)\(Grace et al. 2010;](#)
247 [Fan et al. 2016\).](#)

248 [In our study, we modelled hoverfly-plant interaction networks](#) using a [SEM](#) approach (Fig. 1) with latent
249 variables linking the number of visits per plant-pollinator [species pair](#) to abundance and phenology
250 overlap (PO) data through a first latent table representing probabilities of interactions, another latent
251 table representing the possible interactions between plant and pollinators (as a realization of the
252 aforementioned interaction probability matrix), and a third latent table yielding the expected number
253 of visits per plant-pollinator [species pair](#) (*i.e.* the intensity of interactions). [We used the term latent](#)

Supprimé: dyad

Supprimé: dyad

256 [tables to describe latent variables organized as insect x plant tables, such as the expected number of](#)
257 [visit matrix.](#)

258 In this model, we considered that PO had an effect on possible interactions (I_{ij}) and the number of visits
259 (λ_{ij}) – a longer overlap is intuitively expected to drive a higher probability of interaction and a larger
260 number of visits. Interaction probabilities were also assumed to depend on two random effects (plant
261 and insect species identities, E_i and E_j), to represent heterogeneity of species degrees (*i.e. the number*
262 [of links](#)) in the network. We modelled the [possibility](#) of interaction I_{ij} between insect species i and plant
263 species j (*i.e. $I_{ij} = 1$ when species i and j can interact*) as a Bernoulli random variable of [probability](#) μ_{ij}
264 given by:

$$\text{logit}(\mu_{ij}) = \mu_0 + \mu_{PO}PO_{ij} + E_i + E_j$$

266 where logit is the usual logistic transformation ($\log(x/(1-x))$), μ_0 is the intercept of this relation, μ_{PO} is
267 the coefficient measuring the effect of PO, and E_i and E_j are the random effects associated with insect
268 species i and plant species j respectively.

269 The number of [visits \$V_{ij}\$](#) was assumed to depend on plant and hoverfly abundances, as more abundant
270 species are expected to be more often sampled (and thus more often recorded “in interaction”). [Please](#)
271 [note that we only linked abundances to the number of visits, \$V_{ij}\$, and not to the possibility of interaction](#)
272 [\(\$I_{ij}\$, because the aim of the latter latent table is to capture “forbidden links”, while detectability and](#)
273 [sampling effects are supposed to be captured by the statistical model of the number of interactions.](#)
274 [We integrated species abundances as predictor variables in order to assess the effect of PO on the](#)
275 [number of visits on top of a “null model” that already includes sensible drivers of the numbers of visits,](#)
276 [such as species abundances.](#) V_{ij} was modelled as a Poisson random variable to allow for sampling
277 variability, with a conditional mean λ_{ij} (the intensity of visits that can occur) given by:

$$\log(\lambda_{ij}) = \lambda_0 + \lambda_H A_{H,i} + \lambda_P A_{P,j} + \lambda_{PO} \log(1 + PO_{ij})$$

Supprimé: interactions

Supprimé: The number of visits

281 where λ_0 is the intercept of this relation, λ_H is the coefficient measuring the effect of hoverfly
282 abundance A_H , λ_P is that of plant abundance A_P , and λ_{PO} is the coefficient of the effect of PO.

283 Possible interactions (I_{ij}) and the intensity of visits (λ_{ij}) are multiplied to obtain the unconditional mean
284 number of recorded visits, *i.e.* V_{ij} is then obtained as a Poisson draw of mean $I_{ij} \lambda_{ij}$.

285 Overall we estimated four main parameters: [the effect of phenology overlap on the probability of](#)
286 [interaction \(\$PO \rightarrow I_{ij}, \mu_{PO}\$ \), the effect of phenology overlap on the intensity of interactions \(\$PO \rightarrow \lambda_{ij},\$](#)
287 [\$\lambda_{PO}\$ \)](#), the effect of plant abundance on the intensity of interactions ($A_P \rightarrow \lambda_{ij}$, coefficient λ_P) and the
288 effect of insect (hoverflies) abundance on the intensity of interactions ($A_H \rightarrow \lambda_{ij}, \lambda_H$).

289 We used the `jags` function (R2jags package), which provides an interface from R to the JAGS library
290 for Bayesian data analysis, to estimate model parameters. JAGS (Plummer 2003) uses a Markov Chain
291 Monte Carlo algorithm to generate samples from the posterior distribution of the parameters. We ran
292 two Markov chains with 10^6 iterations per chain to check for model convergence. The code of the
293 model is given in Supplementary Material (Appendix S1 and S2).

294 Model and parameter comparison

295 We estimated the 16 models that included [all combinations of](#) 0 and 4 of the above-mentioned effects
296 to understand which effects were more likely to play a role in the structuring of the network. The
297 goodness-of-fit of these models were compared using the leave-one-out cross-validation criterion
298 (LOO) calculated using the R package `loo` [using Pareto smoothed importance sampling for regularizing](#)
299 [importance weights \(Vehtari et al. 2017\)](#). [The LOO criterion is a fully Bayesian method to compare](#)
300 [models of different complexities and to estimate prediction accuracy using the log-likelihood](#)
301 [evaluated at the posterior simulations of the parameter values \(Vehtari et al. 2017\)](#). Models can thus
302 be ranked according to their LOO scores, with the best model being the one with the lowest LOO value.

303 The LOO criterion is analogous to the classic Akaike and Bayesian Information Criteria, [which are used](#)
304 [to compare frequentist models](#), but can [instead](#) be applied to Bayesian models, without suffering the

Supprimé: the effect of phenology overlap on the intensity of interactions ($PO \rightarrow \lambda_{ij}, \lambda_{PO}$) and the effect of phenology overlap on the probability of interaction ($PO \rightarrow I_{ij}, \mu_{PO}$).

Supprimé: between

309 instability issues of the Deviance Information Criterion [which used to be the main information criterion](#)
310 [for Bayesian models](#) (Vehtari *et al.* 2017). To rank the models, we then calculated the ΔLOO (noted Δ_i)
311 as $\Delta_i = LOO_i - LOO_{min}$ (following Burnham & Anderson 2004), where LOO_{min} is the minimum of the LOO_i
312 values among the 16 models. We used Δ_i to obtain model weights ω_i , following the Akaike weight
313 methodology (Burnham & Anderson 2002):

$$\omega_i = \frac{e^{-\Delta_i/2}}{\sum e^{-\Delta_i/2}}$$

315 We then summed weights (w_H) over all models that incorporated a given focal parameter to ascertain
316 the plausibility of the effect associated to this parameter. We used this sum to evaluate the null
317 hypothesis (H0) that a given factor has no effect on the plant-pollinator interactions by comparing the
318 sum of weights to null expectations, based on the fact that each tested effect is incorporated in exactly
319 half of the tested models. The effect is considered *plausible* when $w_H > 0.5$, *implausible* otherwise,
320 *likely* when $w_H > 0.73$, and *unlikely* when it corresponds to a value of 0.27 or lower, following Massol
321 *et al.* (2007).

322 [Predictive power analysis](#)

323 [We tested the predictive power of the models we built by making predictions for the \$I_{ij}\$ table and](#)
324 [checking their validity using a binarized version of the visit table \$V_{ij}\$. Predictions were obtained by](#)
325 [defining a threshold on interaction probability \$\mu_{ij}\$: values found above the threshold were predicted as](#)
326 [occurring interactions, values below the threshold as no interaction. The threshold probability value](#)
327 [was found by maximizing the sum of model specificity and sensitivity. We computed accuracy statistics](#)
328 [\(sensitivity, specificity, omission rate, area under the ROC curve \[AUC\]\) in two situations: \(i\) when](#)
329 [predicting data for the site that was used to build the model \(self-validation; e.g. predicting interaction](#)
330 [data in the site of Riez based on the model developed for this site\) and \(ii\) when predicting data for](#)
331 [the other site from the same region \(cross-validation; e.g. predicting data for the LAR site based on the](#)
332 [model for the R site\). We performed these analyses using the `SDMTools` package in R. We only used](#)

Supprimé: same

Mis en forme : Soulignement

334 [the set of best models \(LOO < 4\) found for each site to predict the interactions in the other site through](#)
335 [a multimodel averaging approach. We obtained the threshold probability using `optim.tresh`](#)
336 [function with option `max.sensitivity+specificity`.](#)

337 RESULTS

338 Plant-hoverfly networks and phenology overlap

339 At the end of the field campaign we had collected 1584 hoverflies and recorded 1668 interactions
340 between 76 hoverfly species and 117 plant species overall (Table 1). The number of sampled hoverfly
341 and plant species varied between sites and among regions. In Normandie we generally sampled a
342 higher number of hoverflies than in the other two regions (Table 1) [and the maximum number of visits](#)
343 [recorded in the site of FAL was 47 \(between *Helophilus pendulus* and *Scabiosa columbaria*, Fig. S3\) and](#)
344 [in the site of CG was 22 \(between *Eristalis tenax* and *S. columbaria* and between *Sphaerophoria scripta*](#)
345 [and *Leontodon hispidus*, Fig. 3\). We observed the highest diversity of both plants and hoverflies in](#)
346 Occitanie and the lowest diversity of hoverflies in Hauts-de-France. Despite the high species diversity
347 in Occitanie, the [total](#) number of interactions recorded in these sites (BF and F) is not the highest
348 recorded in the field (Table 1): [the maximum number of visits in the site of BF was 10 \(between](#)
349 [Sphaerophoria scripta and Helichrysum stoechas, Fig. S2\) and 12 in the site of F \(between *Syrphus ribesii*](#)
350 [and *Bellis perennis*, Fig. 2\). In the two southern sites we also recorded the lowest connectance values](#)
351 [\(BF: 0.07 and F: 0.08\) of all six sites, with the highest connectance observed in the site of R \(R 0.16; LAR](#)
352 [0.13; CG 0.13; FAL 0.12\). The maximum number of visits recorded in the site of LAR was 12 \(between](#)
353 [Syrphus ribesii and L. hispidus, Fig. S4\) and in the site of R was 17 \(between *Syrirta pipiens* and *Asperula*](#)
354 [cynanchica, Fig. S5\).](#)

355 In spite of differences in diversity and the number of interactions, the overall level of specialization (H2
356 index) did not show a high variation among the 6 networks (range: 0.32 – 0.37). However, we found
357 that the sites in Occitanie (BF and F) had a higher average degree of specialization (d') for both insect
358 (BF 0.63 and F 0.57) and plant species (BF 0.58 and F 0.48). The sites in Occitanie also had a higher

359 modularity (BF 0.51 and F 0.48) than the ones in Normandie (CG 0.34 and FAL 0.23) and Hauts-de-
360 France (LAR 0.37 and R 0.34; Table 1). Given that these statistics only compare 6 sites, none of these
361 assessments can be properly statistically tested, but the importance of the differences among sites is
362 highly suggestive of a difference in average specialization and modularity. We found that plant
363 phenology is generally shorter in all sites than that of hoverflies (Table 1). The phenology overlap was
364 shorter in Occitanie (BF and F) than in the other sites (Table 1).

365 Illustrations of the block clustering provided by the LBM analysis (Latent Block Model) are shown in
366 Fig. 2 and 3 in the main text and in Fig. S2 to S5 in Supplementary Information. We found different
367 numbers of blocks in plants and hoverflies among sites: the BF site had 2 insect blocks and 2 plant
368 blocks (Fig. S2); the F site had 4 of both (Fig. 2); the CG and R sites had 3 blocks for the plants and 4
369 blocks for the insects in (Fig. 3 and S5); the FAL site had 4 plant blocks and 3 insect blocks (Fig. S3); the
370 LAR site had 3 blocks for the plants and 2 for the insects (Fig. S4).

371 Model ranking and comparison of parameters in each site

372 For each site we compared the 16 models using the LOO criterion (Table 2, ΔLOO values). We found
373 that models 1, 2 and 4 had consistently better goodness-of-fit than the others. The model
374 incorporating all effects except the effect of phenological overlap on the probability of interaction
375 (Model 4: $\lambda_{ij} \sim A_H + A_P + \text{PO}$, Table 2) was the best model in the sites of CG, FAL and LAR. In the two
376 southern sites (BF and F), we found that the model incorporating all effects except that of phenological
377 overlap on the intensity of visits (Model 1: $\lambda_{ij} \sim A_H + A_P / I_{ij} \sim \text{PO}$, Table 2), was the best one. The model
378 incorporating all effects (Model 0: $\lambda_{ij} \sim A_H + A_P + \text{PO} / I_{ij} \sim \text{PO}$, Table 2) was found as the best one only in
379 the site of R, but was a suitable model ($\Delta\text{LOO} < 4$) in all the other sites (Table 2). We also compared the
380 sum of model weights of the four parameters among sites (Table 2, [Effects weight](#)). We found that the
381 effect of insect abundance on the intensity of interaction ($A_H \rightarrow \lambda_{ij}$) is always likely (*i.e.* the sum of their
382 weights is always higher than 0.73, Table 2) and of large effect size in all sites (standardised coefficient
383 higher than 1, Fig. 4). Likewise, we found that the effect of plant abundance on the intensity of

Supprimé: Evidence ratio

385 interaction ($A_p \rightarrow \lambda_{ij}$) was always likely and had large effect size in most part of sites, except in the site
386 of F ($w_{ij} = 0.59$, Table 2; standardised coefficient = 0.67, Fig. 4). The effects of phenological overlap on
387 the probability of interaction ($PO \rightarrow I_{ij}$) and the intensity of visits ($PO \rightarrow \lambda_{ij}$), however, had variable
388 plausibility among sites. The effect of phenological overlap on the probability of interaction was *likely*
389 only in half of the sites (Table 2 and Fig. 4). The effect of phenological overlap on the intensity of visits
390 was *not plausible* only in the two southern sites (BF and F) and *plausible* in the other four sites (LAR, R
391 CG and FAL, Table 2 and Fig. 4). In all sites, the standardised coefficients of PO effects were always less
392 than 1, thus showing a low effect size of phenology on interaction probability and intensity (Fig. 4).

Supprimé: ER

393 When assessing the predictive power of the best models, we observed that the sensitivity and
394 specificity values, both for the self-validation and the cross-validation, were higher than 0.5 (Table S2),
395 which means that the interactions predicted by the models are better than predicted by chance. While
396 area under the curve (AUC) values were all higher than 0.75 for self-validation, cross-validation tests
397 yielded intermediate values (AUC between 0.62 and 0.73), reflecting the fact that abundances and
398 phenology are certainly not sufficient to make accurate predictions on the occurrence of plant-
399 pollinator interactions.

Supprimé: suggesting

400 DISCUSSION

401 Latitude affects the seasonality, with advancing species phenologies at higher latitudes, and thus, can
402 be a limiting factor for the phenological coupling of interacting species (Post *et al.* 2018). In this study
403 we explored the effect of phenology overlap on a large network of species interactions in calcareous
404 grasslands and how this effect could vary along a latitudinal gradient in France using empirical data on
405 six plant-hoverfly networks. We identified plants and insects at the species level to build detailed
406 interaction networks and hence avoid spurious generalisation levels. In order to better understand the
407 determinants of variation in species interactions in space and time, we used the latitudinal gradient to
408 consider variations linked to environmental cues and the entire flowering period to allow for seasonal
409 variation (Valverde *et al.* 2016; Pellissier *et al.* 2017). One of the main problems of comparing networks

412 along gradients is the dependence of network metrics on network size (Staniczenko *et al.* 2013;
413 Astegiano *et al.* 2015; Tylianakis & Morris 2017). In this study, [to avoid the problem of comparing](#)
414 [networks with different dimensions, we decided to focus on the determinants of the probability of](#)
415 [interaction and the number of visits, rather than the overall structure.](#) We employed Bayesian
416 Structural Equation Models (SEM) [which is an emergent approach increasingly used to investigate](#)
417 [complex networks of relationship in ecological studies \(Grace *et al.* 2010; Eisenhauer *et al.* 2015; Fan](#)
418 [et al. 2016; Theodorou *et al.* 2017\).](#) In our study we used SEM to link the numbers of visits to [phenology](#)
419 [overlap \(PO\)](#) and [species abundance](#) through latent probabilities of species interaction and expected
420 numbers of visits per plant-pollinator [species pair](#). We tested different models with variable numbers
421 of effects and compared them in each site. [In our models, we used species abundances to construct a](#)
422 [sensible null model to test whether phenology overlap could help explain the probability and intensity](#)
423 [of interactions when the effects of species abundances are already taken into account. In all sites, we](#)
424 [found that models that included both PO and abundances had always better goodness-of-fit than](#)
425 [models that included only abundances. Abundances indeed provided a sensible null model since the](#)
426 [goodness-of-fit of models that did not include abundances were always quite worse than the ones](#)
427 [which did.](#)

428
429 We [also](#) found that in all sites the most important [factor](#) affecting pollinator visits was insect
430 abundance (Table 2). Likewise, we found that plant abundance was also a very important effect in most
431 sites, except in the site of F (Table 2). [Since insect abundances are given by visitation data, it is not](#)
432 [surprising that the intensity of interactions positively depends on these abundances.](#) Species
433 abundance often explain the linkage level in pollination network studies (Olesen *et al.* 2008; Bartomeus
434 *et al.* 2016; Chacoff *et al.* 2017; Pellissier *et al.* 2017) but it is often associated with the length of the
435 phenology to better assess the general properties of the interaction network (Vázquez *et al.* 2009;
436 Olito & Fox 2015). In accordance with this verbal prediction, we indeed found that the best models

Déplacé (insertion) [1]

Supprimé: dyad

Déplacé vers le haut [1]: is an emergent approach increasingly used to investigate complex networks of relationship in ecological studies (Grace *et al.* 2010; Eisenhauer *et al.* 2015; Fan *et al.* 2016; Theodorou *et al.* 2017).

Supprimé: SEM

Supprimé: also

Supprimé: effect

Supprimé: part of

447 incorporated the effect of PO on either the probability or the intensity of interactions (Table 2), [and](#)
448 [the model that only considered species abundance \(model 5 in Table 2\) was not the best one in any](#)
449 [site](#). Phenology overlap generally cannot predict the probability of interaction on its own (Encinas-Viso
450 *et al.* 2012; CaraDonna *et al.* 2017). Our findings do agree with this general predicament since no site
451 favoured a model that only incorporated PO effects and because these effects always display lower
452 effect sizes than the other variables. [However, our objective was not to compare the effect of](#)
453 [phenology overlap to that of species abundance – for such an endeavour, one would need estimates](#)
454 [of species abundances independent of visitation data. Because models which consider the effect of PO](#)
455 [on the intensity and/or probability of interactions are the best models for all sites evinces a clear effect](#)
456 [of PO. In our model, the effect of PO on the probability of interaction and the expected number of](#)
457 [visits also vary along the latitudinal gradient \(Fig. 4\).](#) In general, we observed that southern sites (BF
458 and F) showed shorter plant phenology and phenology overlap (PO) than the other four sites (Table
459 1). In these sites, plant species richness is higher and fewer visits were sampled, probably because the
460 presence of specialist species with short phenophases may increase the number of forbidden or
461 undetected links (Olesen *et al.* 2011; Martín González *et al.* 2012). Conversely, in sites where plant
462 phenology is longer, PO is longer too, as observed in Normandie and Hauts-de-France (CG, FAL, LAR
463 and R, Table 1). Moreover, when plant richness and specialization are lower, a higher number of visits
464 can be observed (Table 1) because generalist species could interact without constraints. Indeed, in
465 Normandie and Hauts-de-France we found that the effect of phenology overlap on the intensity of
466 visits was always likely ($PO \rightarrow \lambda_i$, Table 2) and we observed higher numbers of interactions in the first
467 two/three blocks of insects and plants which also corresponded to blocks with longer PO (Fig. 3, S3, S4
468 and S5). A higher phenological overlap is expected to drive a higher probability of interactions and a
469 larger number of visits (Olesen *et al.* 2011). In Occitanie, we did not find any effect of PO on the number
470 of visits because the more densely visited blocks do not correspond to those with longer phenology
471 overlap. Plant phenology can therefore drive the probability and the intensity of interactions in
472 networks in which plant phenology is shorter, thus suggesting that [hoverflies](#) may undergo selection

Déplacé vers le bas [2]: In our model, the effect of PO on the probability of interaction and the expected number of visits also vary along the latitudinal gradient (Fig. 4).

Déplacé (insertion) [2]

Supprimé: syrphid flies

477 for behavioural flexibility in order to maintain synchrony with their foraging resources (Iler *et al.* 2013;
478 Ogilvie & Forrest 2017).

479 We also found that modularity decreased along the latitudinal gradient, with richer sites (BF and F)
480 displaying higher modularity (as in Sebastián-González *et al.* 2015) [but also the lower connectance](#). In
481 the two southern sites, higher modularity could be related to shorter phenologies and higher
482 proportions of non-overlapping sets of species, which induce some form of temporal short-term
483 specialisation (Lucas *et al.* 2018). However, modularity also seems to be influenced by species
484 abundances and degrees (Schleuning *et al.* 2014), and is expected to increase with link specificity
485 (Morente-López *et al.* 2018). Indeed, in these sites, species blocks match species degrees (Fig. 2 and
486 S2), with generalist and specialist species forming separate blocks among both plants and insects
487 (Martín González *et al.* 2012). With lower modularity and more generalist species, we expect a stronger
488 relationship between phenology and the intensity of interactions because interactions are less
489 influenced by insect preferences and more by seasonal rhythm and flower availability (Dormann *et al.*
490 2017). Thus, different phenophases might correspond to different compartments (Martín González *et al.*
491 *et al.* 2012; Morente-López *et al.* 2018), as observed in CG, FAL, LAR and R where higher overlap
492 corresponded to higher numbers of observed visits. Although phenology improved model fit (Table 2),
493 its effect size was modest (Fig. 4), which suggests that other types of data such as traits and phylogenies
494 might help predict specific interactions. In our study, we did not consider competition among studied
495 insect species or with other group of insects, such as bees which were present in all sites. Different
496 types of pollinators with different abundances could have context-dependent effects on network
497 topology (Valverde *et al.* 2016). [Moreover, in our study we only considered as “true absence” of the](#)
498 [interaction the lack of phenological coupling between species \(i.e. plant and hoverfly species which are](#)
499 [not present at the same moment along the season cannot interact\). We did not consider “false](#)
500 [absences”, i.e. missing links, since not all the potential links among species are recorded in the field](#)
501 [\(Olesen *et al.* 2011\) which may introduce bias in the estimation of the probability of interactions](#)
502 [\(Bartomeus *et al.* 2016; Cirtwill *et al.* 2019\).](#)

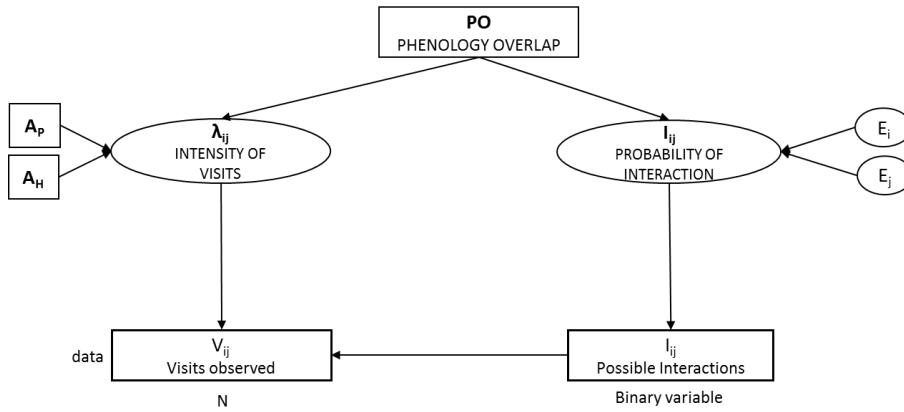
503 To conclude, plant phenology here drives the duration of the phenology overlap between plant and
504 [hoverflies](#), which in turn influences either the probability of interaction or the expected number of
505 visits, as well as network compartmentalization. Longer phenologies correspond to less constrained
506 interactions (lower modularity), shorter phenologies to more constrained interactions (higher
507 modularity), which in turn restrict the number of visits. Phenology overlap alone was not sufficient to
508 explain interactions, as suggested elsewhere (CaraDonna *et al.* 2017). Plant and insect abundances
509 played a substantial role to explain the number of visits (as in Chacoff *et al.* 2017) since abundances
510 may affect partner choice (Trøjelsgaard *et al.* 2015). Our results, and the ability of the method used
511 here to compare different effects on interaction patterns, suggest that the use of Bayesian SEM to
512 compare networks of different sizes is a valuable tool which can help understand plant-pollinator
513 networks (Eisenhauer *et al.* 2015). The use of latent variables can help predict the probability of
514 interaction and the expected number of visits while avoiding circularity – the introduction of plant and
515 insect specific random effects played the role of an implicit “degree” effect. Our results demonstrate
516 the importance of considering differences in plant and insect phenologies to better predict their
517 interactions in pollination networks at different latitudes. The use of morphological traits (*e.g.* tongue
518 length, inter-tegular distance, ...) together with species richness and phylogenies, on top of variables
519 already used, might improve the modelling of interactions and could help better understand some
520 forbidden or missing links in richer communities or considering other pollinators (*e.g.* wild bees).

521 **ACKNOWLEDGEMENTS**

522 Financial support was provided by the ANR ARSENIC project (grant no. 14-CE02-0012), the Region
523 Nord-Pas-de-Calais and the CNRS. We also thank Martin Speight for insect identification, Clément
524 Mazoyer for informatic support and all the students who took part in the field campaign. This work is
525 a contribution to the CPER research project CLIMIBIO. The authors thank the French Ministère de
526 l'Enseignement Supérieur et de la Recherche, the Hauts-de-France Region and the European Funds for
527 Regional Economical Development for their financial support.

528

Supprimé: insects



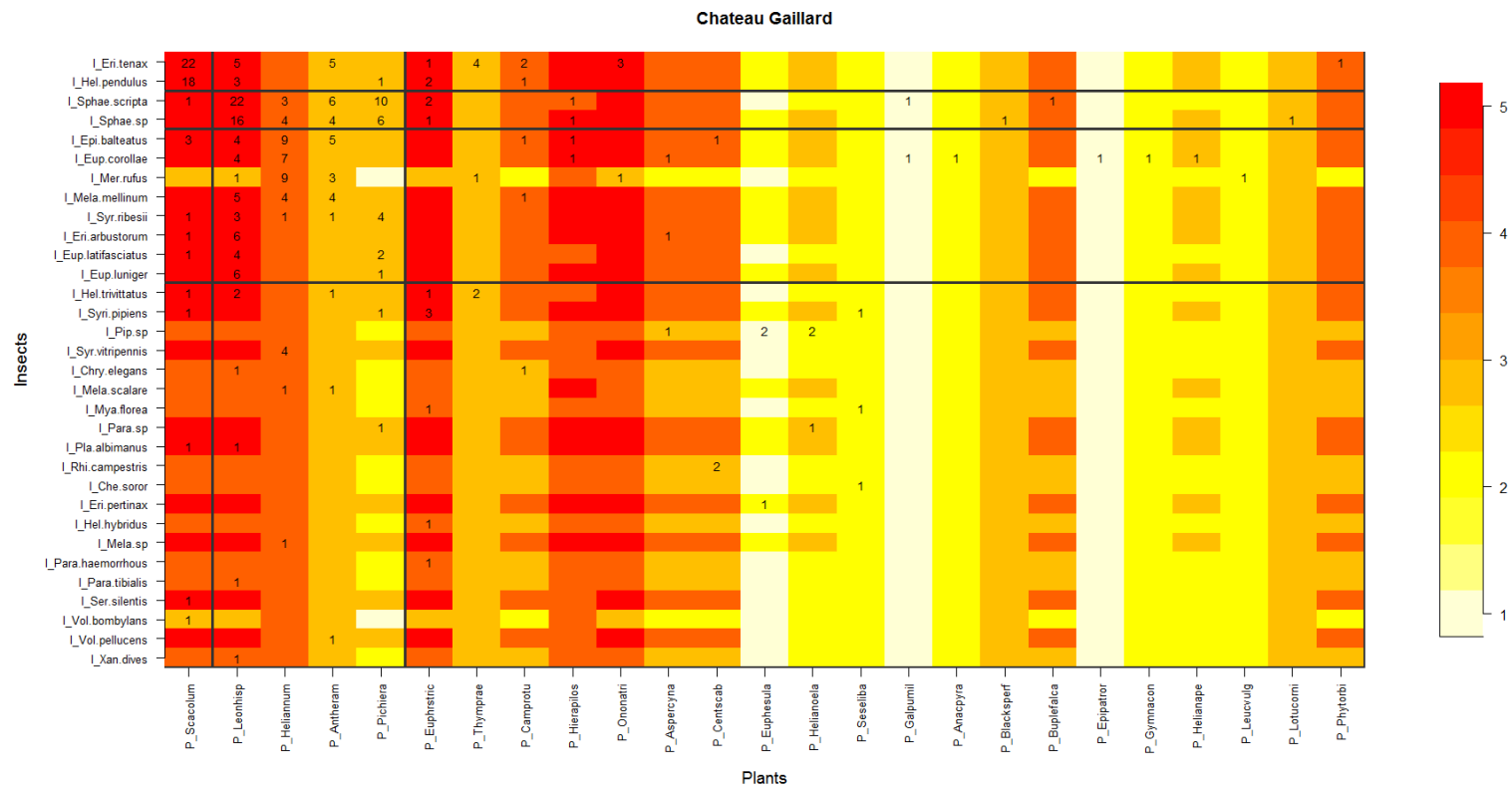
531

532 Figure 1. Summary diagram of the SEM model. We estimated 4 effects: the effect of plant abundance
 533 ($A_p \rightarrow \lambda_{ij}$, coefficient λ_p), the effect of insect (hoverflies) abundance on the intensity of visits ($A_H \rightarrow$
 534 λ_{ij} , λ_H), the effect of phenology overlap on the intensity of visits ($PO \rightarrow \lambda_{ij}$, λ_{PO}) and the effect of
 535 phenology overlap on the probability of interaction ($PO \rightarrow I_{ij}$, μ_{PO}). The phenology overlap (PO) is the
 536 number of phenologically active months that are shared by each pair of insect and plant species along
 537 the season. The intensity of visits (λ_{ij}) and the probability of interaction are latent variables in the
 538 model. Effect-i and effect-p are random effects calculated by the model which represent the insect
 539 and plant species identities. The I_{ij} (Possible interactions) is a binary variable and the V_{ij} (visits
 540 observed) follow a Poisson distribution with an expected value given when the probability of
 541 interaction is predicted as "true". Rectangles represent observed variables while ovals represent
 542 unobserved influences.

543

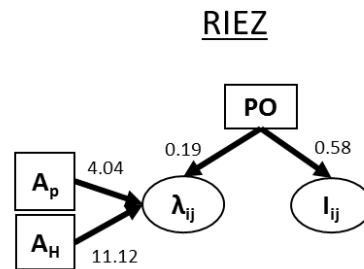
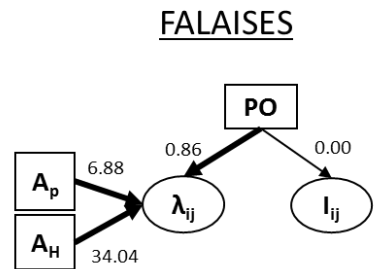
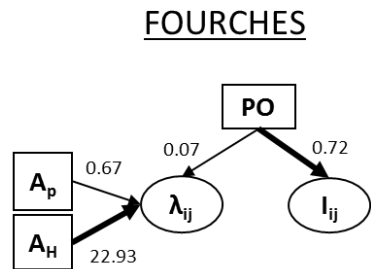
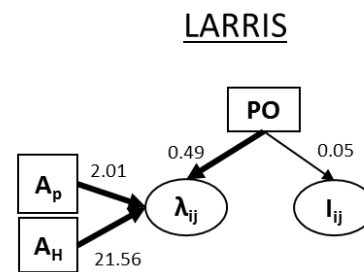
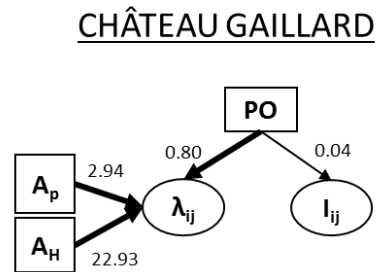
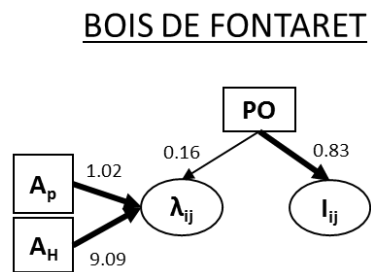
Supprimé: degrees

551 Figure 3. Block clustering provided by LBM in the site of Chateau Gaillard (CG, Normandie) overlaid on a heatmap of species phenology overlap. Insect species
 552 are displayed in rows and plant species in columns, following their degree (number of partners). The blocks of insects and the blocks of plants are separated
 553 by solid black lines. Colours correspond to the number of months that are shared by each pair of plant and insect species (PO, phenology overlap), with higher
 554 PO corresponding to darker colours. Numbers are the number of visits observed in the field for a given plant-insect pair.



555

556 Figure 4. Summary diagram of the best models in all sites. The thickness of the arrows is scaled to Akaike weights (thin ER < 0.73; thick ER > 0.73, cf. Table 2).
 557 Standardised coefficients of the model average (computed based on the Akaike weighted model average) are reported next to the arrows. PO is the phenology
 558 overlap, I_{ij} is the probability of interaction, λ_{ij} is the intensity of visits, A_H and A_P are the hoverflies and plant abundances respectively.



559

560

561 Table 1. Summary table of results obtained in each site (Bois de Fontaret [BF] and Fourches [F] in Occitanie, Château Gaillard [CG] and Falaises [FAL] in
562 Normandie, Larris [LAR] and Riez [R] in Hauts-de-France). $H2'$ and d' indices refer to specialization indices described by Blüthgen *et al.* (2006) and
563 implemented in the R package `bipartite` (Dormann *et al.* 2009). The modularity score was obtained using the `leading-eigenvector` method
564 described by Newman (2006) and implemented in the `igraph` package (Csardi & Nepusz 2006). LBM refers to latent block modelling as implemented in the
565 R package `blockmodels` (Leger *et al.* 2015).

566

Site	Region	Collected data				Specialization index			Species phenology			Modularity analysis	LBM	
		Sampled insects	Insect species	Plant species	Recorded Interactions	$H2'$ index	d' Insects (average + sd)	d' Plants (average + sd)	Insect (average + sd)	Plant (average + sd)	Phenology overlap (PO) (average + sd)	modularity score	blocks I	blocks P
BF	Occitanie	197	40	43	198	0.37	0.63 ± 0.17	0.58 ± 0.17	5.25 ± 1.51	2.14 ± 1.04	1.77 ± 1.03	0.53	2	2
F	Occitanie	223	36	49	286	0.33	0.57 ± 0.18	0.48 ± 0.19	5.61 ± 1.54	2.08 ± 1.13	1.78 ± 1.14	0.48	4	4
CG	Normandie	295	32	25	297	0.34	0.40 ± 0.21	0.47 ± 0.18	6.03 ± 1.00	3.28 ± 1.24	3.02 ± 1.17	0.34	4	3
FAL	Normandie	363	34	30	374	0.32	0.40 ± 0.18	0.41 ± 0.18	6.06 ± 1.13	3.57 ± 1.59	3.23 ± 1.51	0.23	3	4
LAR	Hauts-de-France	220	24	33	220	0.36	0.48 ± 0.19	0.45 ± 0.15	6.38 ± 0.82	3.18 ± 1.38	2.99 ± 1.36	0.37	2	3
R	Hauts-de-France	286	22	29	293	0.32	0.39 ± 0.16	0.40 ± 0.16	5.55 ± 0.74	3.38 ± 1.47	3.11 ± 1.45	0.34	4	3
Total		1584	76	117	1668									

567

568 Table 2. (i) Comparison of SEM models using the leave-one-out cross-validation criterion (LOO); (ii)
 569 evidence ratios (ER) of model effects in each site. (i) Models are ranked depending on the number of
 570 parameters used (from 0 to 4). The best models are the ones with $\Delta\text{LOO}=0$ (underlined and bold
 571 values). The other suitable models are the ones with $\Delta\text{LOO} < 4$ (underlined and italic values). λ_{ij} is the
 572 intensity of visits, I_{ij} is the probability of interaction, A_H is the insect abundance, A_P is the plant
 573 abundance and PO is the phenology overlap. (ii) We compared 4 model effects: $\text{PO} \rightarrow I_{ij}$, effect of the
 574 phenology overlap on the probability of interaction; $\text{PO} \rightarrow \lambda_{ij}$ effect of the phenology overlap on the
 575 intensity of visits; $A_H \rightarrow \lambda_{ij}$ and $A_P \rightarrow \lambda_{ij}$ effects of the hoverflies and plant abundances on the intensity
 576 of interaction. The w_{ij} limits for unlikelihood is 0.27, plausibility 0.5 and likelihood 0.73. Underlined
 577 and bold values represent the likely hypothesis only.

		Sites						
		BF	F	CG	FAL	LAR	R	
Model	Nb of parameters	$\Delta\text{LOO values}$						
0	$\lambda_{ij} \sim A_H + A_P + \text{PO} / I_{ij} \sim \text{PO}$	<u>2.98</u>	<u>2.04</u>	<u>3.54</u>	<u>2.54</u>	<u>2.86</u>	0.00	
1	$\lambda_{ij} \sim A_H + A_P / I_{ij} \sim \text{PO}$	0.00	0.00	36.75	64.04	10.37	<u>2.90</u>	
2	$\lambda_{ij} \sim A_P + \text{PO} / I_{ij} \sim \text{PO}$	8.66	78.23	106.46	184.02	44.60	17.00	
3	$\lambda_{ij} \sim A_H + \text{PO} / I_{ij} \sim \text{PO}$	6.63	<u>1.71</u>	8.09	73.62	11.24	11.42	
4	$\lambda_{ij} \sim A_H + A_P + \text{PO}$	<u>2.86</u>	8.06	0.00	0.00	0.00	<u>2.24</u>	
5	$\lambda_{ij} \sim \text{PO} / I_{ij} \sim \text{PO}$	14.69	73.20	109.85	223.86	55.67	23.09	
6	$\lambda_{ij} \sim A_H / I_{ij} \sim \text{PO}$	<u>1.45</u>	<u>1.31</u>	33.53	119.04	27.23	19.76	
7	$\lambda_{ij} \sim A_P / I_{ij} \sim \text{PO}$	9.84	72.16	156.61	256.04	47.99	21.53	
8	$\lambda_{ij} \sim A_H + \text{PO}$	11.49	8.18	5.25	71.97	10.28	13.80	
9	$\lambda_{ij} \sim A_P + \text{PO}$	10.71	88.67	103.46	182.14	44.36	17.94	
10	$\lambda_{ij} \sim A_H + A_P$	24.36	14.04	36.10	66.82	10.51	4.26	
11	$I_{ij} \sim \text{PO}$	11.78	68.52	154.26	272.98	64.12	32.39	
12	$\lambda_{ij} \sim \text{PO}$	19.99	86.20	108.46	219.66	54.64	25.73	
13	$\lambda_{ij} \sim A_H$	25.58	14.41	36.12	123.30	28.27	22.78	
14	$\lambda_{ij} \sim A_P$	32.99	87.70	157.74	256.39	48.82	22.87	
15	-	34.39	83.89	155.68	274.80	64.78	33.52	
Model effects		<u>Effects weight (w_{ij})</u>						
	$\text{PO} \rightarrow I_{ij}$	0.88	0.98	0.15	0.22	0.20	0.74	
	$\text{PO} \rightarrow \lambda_{ij}$	0.26	0.35	1.00	1.00	0.99	0.79	
	$A_H \rightarrow \lambda_{ij}$	0.99	1.00	1.00	1.00	1.00	1.00	
	$A_P \rightarrow \lambda_{ij}$	0.74	0.59	0.93	1.00	0.99	1.00	

Supprimé: ER

Supprimé: Evidence ratio

578

579

582 **Supporting Information**

583 The following Supporting Information is available for this article:

584 Appendix S1. Model code.

585 Appendix S2. Model script for the 16 models.

586 Appendix S3. Script modularity and latent block model analysis (LBM).

587 Figure S1. Sites location in France.

588 Figure S2. Block clustering provided by LBM in the site of Bois de Fontaret (BF, Occitanie), overlaid on
589 a heatmap of species phenology overlap.

590 Figure S3. Block clustering provided by LBM in the site of Falaises (FAL, Normandie), overlaid on a
591 heatmap of species phenology overlap.

592 Figure S4. Block clustering provided by LBM in the site of Larris (LAR, Hauts-de-France), overlaid on a
593 heatmap of species phenology overlap.

594 Figure S5. Block clustering provided by LBM in the site of Riez (R, Hauts-de-France), overlaid on a
595 heatmap of species phenology overlap.

596 Table S1. Table of transformed plant abundances.

597

598 REFERENCES

- 599 Astegiano, J., Massol, F., Vidal, M.M., Cheptou, P.O. & Guimarães, P.R. (2015). The robustness of
600 plant-pollinator assemblages: Linking plant interaction patterns and sensitivity to pollinator
601 loss. *PLoS One*, 10, e0117243.
- 602 Bartomeus, I., Ascher, J.S., Wagner, D., Danforth, B.N., Colla, S., Kornbluth, S., *et al.* (2011). Climate-
603 associated phenological advances in bee pollinators and bee-pollinated plants. *Proc. Natl. Acad.*
604 *Sci. U. S. A.*, 108, 20645–9.
- 605 Bartomeus, I., Gravel, D., Tylianakis, J.M., Aizen, M.A., Dickie, I.A. & Bernard-Verdier, M. (2016). A
606 common framework for identifying linkage rules across different types of interactions. *Funct.*
607 *Ecol.*, 30, 1894–1903.
- 608 Baude, M., Kunin, W.E., Boatman, N.D., Conyers, S., Davies, N., Gillespie, M.A.K., *et al.* (2016).
609 Historical nectar assessment reveals the fall and rise of floral resources in Britain. *Nature*, 530,
610 85–88.
- 611 Biernacki, C., Celeux, G. & Govaert, G. (2000). Assessing a mixture model for clustering with
612 integrated completed likelihood. *IEEE Trans. Pattern Anal. Mach. Intell.*, 22, 719–725.
- 613 Blüthgen, N., Menzel, F. & Blüthgen, N. (2006). Measuring specialization in species interaction
614 networks. *BMC Ecol.*, 6, 9.
- 615 Branquart, E. & Hemptinne, J. (2000). Selectivity in the exploitation of floral resources by hoverflies
616 (Diptera: Syrphinae). *Ecography (Cop.)*, 23, 732–742.
- 617 Burnham, K.P. & Anderson, D.R. (2002). *Model Selection and Multimodel Inference A Practical*
618 *Information-Theoretic Approach*. 2nd Editio. Springer-Verlag, New York.
- 619 Burnham, K.P. & Anderson, D.R. (2004). Multimodel inference: Understanding AIC and BIC in model
620 selection. *Sociol. Methods Res.*, 33, 261–304.
- 621 CaraDonna, P.J., Petry, W.K., Brennan, R.M., Cunningham, J.L., Bronstein, J.L., Waser, N.M., *et al.*
622 (2017). Interaction rewiring and the rapid turnover of plant – pollinator networks. *Ecol. Lett.*,
623 20, 385–394.
- 624 Chacoff, N.P., Resasco, J. & Vázquez, D.P. (2017). Interaction frequency, network position, and the
625 temporal persistence of interactions in a plant–pollinator network. *Ecology*, 99, 21–28.
- 626 Cirtwill, A.R., Eklof, A., Roslin, T., Wootton, K. & Gravel, D. (2019). A quantitative framework for
627 investigating the reliability of network construction. *Methods Ecol. Evol.*, 10, 902–911.
- 628 Colley, M.R. & Luna, J.M. (2000). Relative attractiveness of potential beneficial insectary plants to
629 aphidophagous hoverflies (Diptera: Syrphidae). *Environ. Entomol.*, 29, 1054–1059.
- 630 Cowgill, S.E., Wratten, S.D. & Sotherton, N.W. (1993). The selective use of floral resources by the
631 hoverfly *Episyrphus balteatus* (Diptera: Syrphidae) on farmland. *Ann. Appl. Biol.*, 122, 223–231.
- 632 Csardi, G. & Nepusz, T. (2006). The igraph software package for complex network research.
633 *InterJournal, Complex Sy*, 1695.
- 634 D’Amen, M., Birtele, D., Zapponi, L. & Hardersen, S. (2013). Patterns in diurnal co-occurrence in an
635 assemblage of hoverflies (Diptera: Syrphidae). *Eur. J. Entomol.*, 110, 649–656.
- 636 Daudin, J.J., Picard, F. & Robin, S. (2008). A mixture model for random graphs. *Stat. Comput.*, 18,
637 173–183.

638 Devoto, M., Medan, D. & Montaldo, N.H. (2005). Patterns of interaction between plants and
639 pollinators along an environmental gradient. *Oikos*, 109, 461–472.

640 Dormann, C.F., Fründ, J., Blüthgen, N. & Gruber, B. (2009). Indices, graphs and null models: analyzing
641 bipartite ecological networks. *Open Ecol. J.*, 2, 7–24.

642 Dormann, C.F., Fründ, J. & Schaefer, H.M. (2017). Identifying causes of patterns in ecological
643 networks: opportunities and limitations. *Annu. Rev. Ecol. Evol. Syst.*, 48, 12–20.

644 Eisenhauer, N., Bowker, M.A., Grace, J.B. & Powell, J.R. (2015). From patterns to causal
645 understanding: Structural equation modeling (SEM) in soil ecology. *Pedobiologia (Jena)*, 58, 65–
646 72.

647 Encinas-Viso, F., Revilla, T.A. & Etienne, R.S. (2012). Phenology drives mutualistic network structure
648 and diversity. *Ecol. Lett.*, 15, 198–208.

649 Fan, Y., Chen, J., Shirkey, G., John, R., Wu, S.R., Park, H., *et al.* (2016). Applications of structural
650 equation modeling (SEM) in ecological studies: an updated review. *Ecol. Process*.

651 Fortuna, M.A., Stouffer, D.B., Olesen, J.M., Jordano, P., Mouillot, D., Krasnov, B.R., *et al.* (2010).
652 Nestedness versus modularity in ecological networks: Two sides of the same coin? *J. Anim.*
653 *Ecol.*, 79, 811–817.

654 Grace, J.B. (2006). *Structural Equation Modeling and Natural Systems*. Cambridge University Press,
655 New York.

656 Grace, J.B., Anderson, T.M., Olf, H. & Scheiner, S.M. (2010). On the specification of structural
657 equation models for ecological systems. *Ecol. Monogr.*, 80, 67–87.

658 Grace, J.B. & Bollen, K.A. (2008). Representing general theoretical concepts in structural equation
659 models: The role of composite variables. *Environ. Ecol. Stat.*, 15, 191–213.

660 Hutchings, M.J., Robbirt, K.M., Roberts, D.L. & Davy, A.J. (2018). Vulnerability of a specialized
661 pollination mechanism to climate change revealed by a 356-year analysis. *Bot. J. Linn. Soc.*, 186,
662 498–509.

663 Iler, A., Inouye, D., Høye, T., Miller-Rushing, A., Burkle, L. & Johnston, E. (2013). Maintenance of
664 temporal synchrony between syrphid flies and floral resources despite differential phenological
665 responses to climate. *Glob. Chang. Biol.*, 19, 2348–2359.

666 Jauker, F. & Wolters, V. (2008). Hover flies are efficient pollinators of oilseed rape. *Oecologia*, 156,
667 819–823.

668 Klecka, J., Biella, P. & Klecka, J. (2018a). Flower visitation by hoverflies (Diptera : Syrphidae) in a
669 temperate plant-pollinator network. *PeerJ Preprints*, 19, 780–785.

670 Klecka, J., Hadrava, J. & Koloušková, P. (2018b). Vertical stratification of plant–pollinator interactions
671 in a temperate grassland. *PeerJ*, 6, e4998.

672 Leger, J.B., Daudin, J.J. & Vacher, C. (2015). Clustering methods differ in their ability to detect
673 patterns in ecological networks. *Methods Ecol. Evol.*, 6, 474–481.

674 Lucas, A., Bodger, O., Brosi, B.J., Ford, C.R., Forman, D.W., Greig, C., *et al.* (2018). Generalisation and
675 specialisation in hoverfly (Syrphidae) grassland pollen transport networks revealed by DNA
676 metabarcoding. *J. Anim. Ecol.*, 87, 1008–1021.

677 Lunau, K. (2014). Visual ecology of flies with particular reference to colour vision and colour

678 preferences. *J. Comp. Physiol. A Neuroethol. Sensory, Neural, Behav. Physiol.*, 200, 497–512.

679 Van Der Maarel, E. (1975). The Braun-Blanquet approach in perspective. *Veget*, 30, 213–219.

680 Van Der Maarel, E. (1979). Arrhenatheretum, Classification, Combined estimation, Cover-abundance
681 scale, Ordination, Phytosociology, Salt marsh, Similarity, Transformation. *Vegetatio*, 39, 97–114.

682 Martín González, A.M., Allesina, S., Rodrigo, A. & Bosch, J. (2012). Drivers of compartmentalization in
683 a Mediterranean pollination network. *Oikos*, 121, 2001–2013.

684 Massol, F., David, P., Gerdeaux, D. & Jarne, P. (2007). The influence of trophic status and large-scale
685 climatic change on the structure of fish communities in Perialpine lakes. *J. Anim. Ecol.*, 76, 538–
686 551.

687 Memmott, J., Craze, P.G., Waser, N.M. & Price, M. V. (2007). Global warming and the disruption of
688 plant-pollinator interactions. *Ecol. Lett.*, 10, 710–717.

689 Miller-Struttman, N.E., Geib, J.C., Franklin, J.D., Kevan, P.G., Holdo, R.M., Ebert-may, D., *et al.*
690 (2015). Functional mismatch in a bumble bee pollination mutualism under climate change.
691 *Science*, 349, 1541–4.

692 Morente-López, J., Lara-Romero, C., Ornos, C. & Iriondo, J.M. (2018). Phenology drives species
693 interactions and modularity in a plant - flower visitor network. *Sci. Rep.*, 8, 9386.

694 Mucina, L., Schaminée, J.H.J. & Rodwell, J.S. (2000). Common data standards for recording relevés in
695 field survey for vegetation classification. *J. Veg. Sci.*, 11, 769–772.

696 Newman, M.E.J. (2006). Finding community structure in networks using the eigenvectors of matrices.
697 *Phys. Rev. E - Stat. Nonlinear, Soft Matter Phys.*, 74, 036104.

698 Ogilvie, J.E. & Forrest, J.R. (2017). Interactions between bee foraging and floral resource phenology
699 shape bee populations and communities. *Curr. Opin. Insect Sci.*

700 Olesen, J.M., Bascompte, J., Dupont, Y.L., Elberling, H., Rasmussen, C. & Jordano, P. (2011). Missing
701 and forbidden links in mutualistic networks. *Proc. Biol. Sci.*, 278, 725–732.

702 Olesen, J.M., Bascompte, J., Elberling, H. & Jordano, P. (2008). Temporal dynamics in a pollination
703 network. *Ecology*, 89, 1573–1582.

704 Olito, C. & Fox, J.W. (2015). Species traits and abundances predict metrics of plant-pollinator network
705 structure, but not pairwise interactions. *Oikos*, 124, 428–436.

706 Parmesan, C. (2007). Influences of species, latitudes and methodologies on estimates of phenological
707 response to global warming. *Glob. Chang. Biol.*, 13, 1860–1872.

708 Pellissier, L., Albouy, C., Bascompte, J., Farwig, N., Graham, C., Loreau, M., *et al.* (2017). Comparing
709 species interaction networks along environmental gradients. *Biol. Rev.*, 93, 785–800.

710 Plummer, M. (2003). JAGS: a program for analysis of Bayesian graphical models using Gibbs sampling.

711 Poisot, T. & Gravel, D. (2014). When is an ecological network complex? Connectance drives degree
712 distribution and emerging network properties. *PeerJ*, 2, e251.

713 Post, E., Steinman, B.A. & Mann, M.E. (2018). Acceleration of phenological advance and warming
714 with latitude over the past century. *Sci. Rep.*, 8, 3927.

715 R Core Team. (2018). R: A language and environment for statistical computing. R Foundation for
716 Statistical Computing, Vienna, Austria. URL <https://www.R-project.org/>.

- 717 Rader, R., Edwards, W., Westcott, D.A., Cunningham, S.A. & Howlett, B.G. (2011). Pollen transport
718 differs among bees and flies in a human-modified landscape. *Divers. Distrib.*, 17, 519–529.
- 719 Rafferty, N.E. (2017). Effects of global change on insect pollinators: multiple drivers lead to novel
720 communities. *Curr. Opin. Insect Sci.*
- 721 Rafferty, N.E., CaraDonna, P.J. & Bronstein, J.L. (2015). Phenological shifts and the fate of
722 mutualisms. *Oikos*, 124, 14–21.
- 723 Schleuning, M., Fru, J., Klein, A., Abrahamczyk, S., Albrecht, M., Andersson, G.K.S., *et al.* (2012).
724 Report Specialization of Mutualistic Interaction Networks Decreases toward Tropical Latitudes,
725 1925–1931.
- 726 Schleuning, M., Ingmann, L., Strauß, R., Fritz, S.A., Dalsgaard, B., Matthias Dehling, D., *et al.* (2014).
727 Ecological, historical and evolutionary determinants of modularity in weighted seed-dispersal
728 networks. *Ecol. Lett.*, 17, 454–463.
- 729 Sebastián-González, E., Dalsgaard, B., Sandel, B. & Guimarães, P.R. (2015). Macroecological trends in
730 nestedness and modularity of seed-dispersal networks: Human impact matters. *Glob. Ecol.*
731 *Biogeogr.*, 24, 293–303.
- 732 Speight, M.C.D., Castella, E., Sarthou, J.-P. & Vanappelghem, C. (2016). StN 2016. In: Syrph the Net on
733 CD, Issue 11. Speight, M.C.D., Castella, E., Sarthou, J.-P. & Vanappelghem, C. (Eds.) Syrph the
734 Net Publications, Dublin.
- 735 Staniczenko, P.P.A., Kopp, J.C. & Allesina, S. (2013). The ghost of nestedness in ecological networks.
736 *Nat. Commun.*, 4, 1391–1396.
- 737 Staniczenko, P.P.A., Lewis, O.T., Tylianakis, J.M., Albrecht, M., Coudrain, V., Klein, A.-M., *et al.* (2017).
738 Predicting the effect of habitat modification on networks of interacting species. *Nat. Commun.*,
739 8.
- 740 Theodorou, P., Albig, K., Radzevičiūtė, R., Settele, J., Schweiger, O., Murray, T.E., *et al.* (2017). The
741 structure of flower visitor networks in relation to pollination across an agricultural to urban
742 gradient. *Funct. Ecol.*, 31, 838–847.
- 743 Trøjsgaard, K., Jordano, P., Carstensen, D.W. & Olesen, J.M. (2015). Geographical variation in
744 mutualistic networks: Similarity, turnover and partner fidelity. *Proc. R. Soc. B Biol. Sci.*, 282,
745 20142925.
- 746 Tylianakis, J.M. & Morris, R.J. (2017). Ecological networks across environmental gradients. *Annu. Rev.*
747 *Ecol. Evol. Syst.*, 48, 25–48.
- 748 Valverde, J., Gómez, J.M. & Perfectti, F. (2016). The temporal dimension in individual-based plant
749 pollination networks. *Oikos*, 125, 468–479.
- 750 Vázquez, D.P., Chacoff, N.P. & Cagnolo, L. (2009). Evaluating multiple determinants of the structure
751 of plant-animal mutualistic networks. *Ecology*, 90, 2039–2046.
- 752 Vehtari, A., Gelman, A. & Gabry, J. (2017). Practical Bayesian model evaluation using leave-one-out
753 cross-validation and WAIC. *Stat. Comput.*, 27, 1413–1432.
- 754 Westphal, C., Bommarco, R., Carré, G., Lamborn, E., Morison, M., Petanidou, T., *et al.* (2008).
755 Measuring bee diversity in different European habitats and biogeographic regions. *Ecol.*
756 *Monogr.*, 78, 653–671.
- 757 Willmer, P. (2012). Ecology: Pollinator-plant synchrony tested by climate change. *Curr. Biol.*, 22,

758

R131-R132.

759

760

Supplementary Information

761 Does phenology explain plant-pollinator interactions at different latitudes? An assessment of its
762 explanatory power in plant-hoverfly networks in French calcareous grasslands

763 N. de Manincor^{1*}, N. Hautekeete¹, Y. Piquot¹, B. Schatz², C. Vanappelghem³, F. Massol^{1,4}

764 ¹ Université de Lille, CNRS, UMR 8198 - Evo-Eco-Paleo, 59000 Lille, France

765 ² CEFE, EPHE-PSL, CNRS, University of Montpellier, University of Paul Valéry Montpellier 3, IRD,
766 Montpellier, France

767 ³ Conservatoire d'espaces naturels Nord et du Pas-de-Calais, 160 rue Achille Faniens - ZA de la Haye,
768 62190 LILLERS

769 ⁴ Univ. Lille, CNRS, Inserm, CHU Lille, Institut Pasteur de Lille, U1019 - UMR 8204 - CIIL - Center for
770 Infection and Immunity of Lille, F-59000 Lille, France

771

772 Natasha de Manincor ORCID: 0000-0001-9696-125X

773 Nina Hautekeete ORCID: 0000-0002-6071-5601

774 Yves Piquot ORCID: 0000-0001-9977-8936

775 Bertrand Schatz ORCID: 0000-0003-0135-8154

776 François Massol ORCID: 0000-0002-4098-955X

777

778 *Corresponding author

779

780 E-mail adresses: natasha.de-manincor@univ-lille.fr, francois.massol@univ-lille.fr,
781 nina.hautekeete@univ-lille.fr, yves.piquot@univ-lille.fr, Bertrand.SCHATZ@cefe.cnrs.fr,
782 cedric.vanappelghem@espaces-naturels.fr

Code de champ modifié

Code de champ modifié

Code de champ modifié

Code de champ modifié

Code de champ modifié

Code de champ modifié

Code de champ modifié

Mis en forme : Anglais (Royaume-Uni)

783 **Appendix S1: Model Code**

784 The model code (in JAGS language) given in this supplementary material refers to the “model Z0” which
785 considers all four parameters (model effects, Table 2 in the main text). Overall, we estimated 16
786 models that included between 0 and 4 of the above-mentioned effects. To create the code for these
787 other models, parameters should be removed following the order in the Tab. 2. The four parameters
788 tested in the model are: (i) alpha: effect of the phenology overlap (cooc) on the probability of
789 interaction; (ii) epsilon: effect of the phenology overlap on the intensity of visits; (iii) gamma: effect of
790 the insect abundances (ab_I) on the intensity of visits; and (iv) delta: effect of the plant abundances
791 (ab_P) on the intensity of visits.

```
792  
793 model  
794 {  
795   for( i in 1 : dim1 ) {  
796     for( p in 1 : dim2 ) {  
797       inter[i , p] ~ dbern(mu[i , p])  
798       logit(mu[i , p]) <- beta + alpha*cooc[i , p] + effet_I[i] + effet_P[p]  
799       lambda[i,p] <- exp(theta[i,p])  
800       theta[i,p] <- theta0 + gamma*ab_I[i] + delta*ab_P[p] + epsilon*log(1+cooc[i,p])  
801       visit[i,p] ~ dpois( inter[i,p]*lambda[i,p] )  
802       loglik[i,p] <- log(ifelse(visit[i,p]==0,1-mu[i,p]+mu[i , p]*dpois(visit[i,p],lambda[i,p]),mu[i ,  
803 p]*dpois(visit[i,p],lambda[i,p])))  
804     }  
805   }  
806  
807   for( i in 1 : dim1 ) {  
808     effet_I[i] ~ dnorm( 0.0,tau_I)
```

```
809 }
810
811 for( p in 1 : dim2 ) {
812   effet_P[p] ~ dnorm( 0.0,tau_P)
813 }
814
815   tau_I ~ dexp( 10)
816   tau_P ~ dexp( 10)
817   alpha ~ dnorm(0,0.01)
818   beta ~ dnorm(0,0.01)
819   theta0 ~ dnorm(0,0.01)
820   gamma ~ dnorm(0,0.01)
821   delta ~ dnorm(0,0.01)
822   epsilon ~ dnorm(0,0.01)
823 }
824
```

Code de champ modifié

Mis en forme : Anglais (Royaume-Uni)

825 **Appendix 2: Model script for the 16 models – LOO values**

826 The following generic script was applied to all the study sites using all 16 models. The script is separated
827 in three blocks which communicate among them: the script options, the model definitions and the
828 execution (model inference). We defined three options to set (i) the name of the directory (-d), (ii) the
829 site (-s) and (iii) the type of model (-m).

830 We used, as an example, the information for the site of Bois de Fontaret (BF).

831 Exemple: Rscript (name) "script-SEMLOO_generique.R" "-d o-BFs-2016" "-s BFs"

832 In order to calculate the standardised coefficients for each parameters used, at the end of the third
833 block, we added the functions to get the parameter values for each site and each model.

834 ##### BLOCK 1 – SCRIPT OPTION #####

835 library(optparse)

836 option_list = list(

837 make_option(c("-d", "--dir"), type="character", default=NULL, help="directory",

838 metavar="character"),

839 make_option(c("-s", "--site"), type="character", default=NULL, help="site name",

840 metavar="character"),

841 make_option(c("-m", "--modele"), type="character", default="all", help="modele name",

842 metavar="character"))

843 opt_parser = OptionParser(option_list=option_list);

844 opt = parse_args(opt_parser);

845 site<-opt\$site

846 dossier<-opt\$dir

847 ##### Librairies #####

848 library(bipartite)

849 library(vegan)

850 library(igraph)

```

851 library(magrittr)
852 library(dummies)
853 library(MuMIn)
854 library(rjags)
855 library(boot)
856 library(R2jags)
857 library(coda)
858 library(lattice)
859 library(ggplot2)
860 library(loo)
861 library(matrixStats)
862 ##### Function to record the LOO values #####
863 write_values<-function(x, f, app)
864 {
865     write.table(x, append=app, file=f, sep="\t", row.names=T, col.names=T, quote=F)
866 }
867 ##### BLOCK 2 – MODEL FUNCTIONS #####
868 #Model function and model initialization: one function for each model from model Z15, with 0
869 parameters, to Z00 with all the parameters#
870 ### MODEL Z015
871 mZ015<-function(){
872     init.funZ015 <-function(){
873         list("tau_I" = rexp(1,10), "tau_P" = rexp(1,10), "beta" = rnorm(1,0,1), "theta0" =
874 rnorm(1,0,1), "effet_I"=rnorm(dim1,0,1),"effet_P"=rnorm(dim2,0,1), "inter"=inter0)
875     }

```

```

876     mod.Z015<<-jags(inits=init.funZ015,model.file = "modelZ015_code.txt",data =
877 list("visit","dim1","dim2"),parameters.to.save =
878 c("mu","effet_I","effet_P","tau_I","tau_P","beta","theta0", "loglik"),n.chains = 1, n.iter=1000000,
879 n.burnin = 250000, n.thin = 250)
880     mod.Z015.mcmc<-as.mcmc(mod.Z015)
881     mZ015<-mod.Z015$BUGSoutput$sims.list
882     mZ015.deviance<-mZ015$deviance
883     mZ015.loglik<-mZ015$loglik
884     dimSEM<-dim(mZ015.loglik)[1]
885     list.mZ015<-sapply(1:dimSEM,function(x) matrix(mZ015.loglik[x,,],nrow=dim1*dim2))
886     list.tmZ015<-t(list.mZ015))
887     mZ015.loo<-loo(list.tmZ015)
888     loo_file<-paste(dossier, "/", site, "_Z015_loo.txt", sep="")
889     write_values("mZ015", app=F, loo_file)
890     mZ015_loo_pointwise<-mZ015.loo$pointwise
891     mZ015_loo_pareto_k<-mZ015.loo$pareto_k
892     mZ015.loo$pareto_k<-NULL
893     mZ015.loo$pointwise<-NULL
894     write_values(as.matrix(mZ015.loo), app=T, loo_file)
895     save.image(paste(dossier, "/", site, "_Z015.RData", sep=""))
896 }
897 ### MODEL Z014
898 mZ014<-function(){
899     init.funZ014 <-function(){
900     list("tau_I" = rexp(1,10), "tau_P" = rexp(1,10), "beta" = rnorm(1,0,1), "delta" = rnorm(1,0,1),
901 "theta0" = rnorm(1,0,1), "effet_I"=rnorm(dim1,0,1),"effet_P"=rnorm(dim2,0,1), "inter"=inter0)

```

```

902     }
903     mod.Z014<-jags(inits=init.funZ014,model.file = "modelZ014_code.txt",data =
904 list("visit","ab_P","dim1","dim2"),parameters.to.save =
905 c("mu","effet_I","effet_P","tau_I","tau_P","delta","beta","theta0","loglik"),n.chains = 1,
906 n.iter=1000000, n.burnin = 250000, n.thin = 250)
907     mod.Z014.mcmc<-as.mcmc(mod.Z014)
908     mZ014<-mod.Z014$BUGSoutput$sims.list
909     mZ014.deviance<-mZ014$deviance
910     mZ014.loglik<-mZ014$loglik
911     dimSEM<-dim(mZ014.loglik)[1]
912     list.mZ014<-sapply(1:dimSEM,function(x) matrix(mZ014.loglik[x,,],nrow=dim1*dim2))
913     list.tmZ014<-(t(list.mZ014))
914     mZ014.loo<-loo(list.tmZ014)
915     mZ014.loo
916     loo_file<-paste(dossier, "/", site, "_Z014_loo.txt", sep="")
917     write_values("mZ014", app=T, loo_file)
918     mZ014_loo_pointwise<-mZ014.loo$pointwise
919     mZ014_loo_pareto_k<-mZ014.loo$pareto_k
920     mZ014.loo$pareto_k<-NULL
921     mZ014.loo$pointwise<-NULL
922     write_values(as.matrix(mZ014.loo), app=T, loo_file)
923     save.image(paste(dossier, "/", site, "_Z014.RData", sep=""))
924 }
925 ### MODEL Z013
926 mZ013<-function(){
927     init.funZ013 <-function(){

```

Code de champ modifié

Mis en forme : Anglais (Royaume-Uni)


```

928     list("tau_I" = rexp(1,10), "tau_P" = rexp(1,10), "beta" = rnorm(1,0,1), "gamma" =
929 rnorm(1,0,1), "theta0" = rnorm(1,0,1), "effet_I"=rnorm(dim1,0,1),"effet_P"=rnorm(dim2,0,1),
930 "inter"=inter0)
931   }
932   mod.Z013<-jags(inits=init.funZ013,model.file = "modelZ013_code.txt",data =
933 list("visit","ab_I","dim1","dim2"),parameters.to.save =
934 c("mu","effet_I","effet_P","tau_I","tau_P","gamma","beta","theta0","loglik"),n.chains = 1,
935 n.iter=1000000, n.burnin = 250000, n.thin = 250)
936   mod.Z013.mcmc<-as.mcmc(mod.Z013)
937   mZ013<-mod.Z013$BUGSoutput$sims.list
938   mZ013.deviance<-mZ013$deviance
939   mZ013.loglik<-mZ013$loglik
940   dimSEM<-dim(mZ013.loglik)[1]
941   list.mZ013<-sapply(1:dimSEM,function(x) matrix(mZ013.loglik[x,,],nrow=dim1*dim2))
942   list.tmZ013<-(t(list.mZ013))
943   mZ013.loo<-loo(list.tmZ013)
944   mZ013.loo
945   loo_file<-paste(dossier, "/", site, "_Z013_loo.txt", sep="")
946   write_values("mZ013", app=T, loo_file)
947   mZ013_loo_pointwise<-mZ013.loo$pointwise
948   mZ013_loo_pareto_k<-mZ013.loo$pareto_k
949   mZ013.loo$pareto_k<-NULL
950   mZ013.loo$pointwise<-NULL
951   write_values(as.matrix(mZ013.loo), app=T, loo_file)
952   save.image(paste(dossier, "/", site, "_Z013.RData", sep=""))
953 }

```

```

954   ### MODEL Z012
955   mZ012<-function(){
956       init.funZ012 <-function(){
957           list("tau_I" = rexp(1,10), "tau_P" = rexp(1,10), "beta" = rnorm(1,0,1), "theta0" =
958   rnorm(1,0,1), "epsilon" = rnorm(1,0,1), "effet_I"=rnorm(dim1,0,1),"effet_P"=rnorm(dim2,0,1),
959   "inter"=inter0)
960       }
961       mod.Z012<<-jags(inits=init.funZ012,model.file = "modelZ012_code.txt",data =
962   list("cooc","visit","dim1","dim2"),parameters.to.save =
963   c("mu","effet_I","effet_P","tau_I","tau_P","beta","theta0","epsilon","loglik"),n.chains = 1,
964   n.iter=1000000, n.burnin = 250000, n.thin = 250)
965       mod.Z012.mcmc<-as.mcmc(mod.Z012)
966       mZ012<-mod.Z012$BUGSoutput$sims.list
967       mZ012.deviance<-mZ012$deviance
968       mZ012.loglik<-mZ012$loglik
969       dimSEM<-dim(mZ012.loglik)[1]
970       list.mZ012<-sapply(1:dimSEM,function(x) matrix(mZ012.loglik[x,,],nrow=dim1*dim2))
971       list.tmZ012<-t(list.mZ012))
972       mZ012.loo<-loo(list.tmZ012)
973       mZ012.loo
974       loo_file<-paste(dossier, "/", site, "_Z012_loo.txt", sep="")
975       write_values("mZ012", app=T, loo_file)
976       mZ012_loo_pointwise<-mZ012.loo$pointwise
977       mZ012_loo_pareto_k<-mZ012.loo$pareto_k
978       mZ012.loo$pareto_k<-NULL
979       mZ012.loo$pointwise<-NULL

```

```

980     write_values(as.matrix(mZ012.loo), app=T, loo_file)
981     save.image(paste(dossier, "/", site, "_Z012.RData", sep=""))
982 }
983 ### MODEL Z011
984 mZ011<-function(){
985     init.funZ011 <-function(){
986         list("tau_I" = rexp(1,10), "tau_P" = rexp(1,10), "alpha" = 0.1,"beta" = rnorm(1,0,1), "theta0"
987 = rnorm(1,0,1), "effet_I"=rnorm(dim1,0,1),"effet_P"=rnorm(dim2,0,1), "inter"=inter0)
988     }
989     mod.Z011<<-jags(inits=init.funZ011,model.file = "modelZ011_code.txt",data =
990 list("cooc","visit","dim1","dim2"),parameters.to.save =
991 c("mu","effet_I","effet_P","tau_I","tau_P","alpha","beta","theta0","loglik"),n.chains = 1,
992 n.iter=1000000, n.burnin = 250000, n.thin = 250)
993     mod.Z011.mcmc<-as.mcmc(mod.Z011)
994     mZ011<-mod.Z011$BUGSoutput$sims.list
995     mZ011.deviance<-mZ011$deviance
996     mZ011.loglik<-mZ011$loglik
997     dimSEM<-dim(mZ011.loglik)[1]
998     list.mZ011<-sapply(1:dimSEM,function(x) matrix(mZ011.loglik[x,,],nrow=dim1*dim2))
999     list.tmZ011<-(t(list.mZ011))
1000     mZ011.loo<-loo(list.tmZ011)
1001     mZ011.loo
1002     loo_file<-paste(dossier, "/", site, "_Z011_loo.txt", sep="")
1003     write_values("mZ011", app=T, loo_file)
1004     mZ011_loo_pointwise<-mZ011.loo$pointwise
1005     mZ011_loo_pareto_k<-mZ011.loo$pareto_k

```

```

1006     mZ011.loo$pareto_k<-NULL
1007     mZ011.loo$pointwise<-NULL
1008     write_values(as.matrix(mZ011.loo), app=T, loo_file)
1009     save.image(paste(dossier, "/", site, "_Z011.RData", sep=""))
1010 }
1011 ### MODEL Z010
1012 mZ010<-function(){
1013     init.funZ010 <-function(){
1014         list("tau_l" = rexp(1,10), "tau_P" = rexp(1,10), "beta" = rnorm(1,0,1), "gamma" =
1015 rnorm(1,0,1), "delta" = rnorm(1,0,1), "theta0" = rnorm(1,0,1),
1016 "effet_l"=rnorm(dim1,0,1),"effet_P"=rnorm(dim2,0,1), "inter"=inter0)
1017     }
1018     mod.Z010<<-jags(inits=init.funZ010,model.file = "modelZ010_code.txt",data =
1019 list("visit","ab_l","ab_P","dim1","dim2"),parameters.to.save =
1020 c("mu","effet_l","effet_P","tau_l","tau_P","gamma","delta","beta","theta0","loglik"),n.chains = 1,
1021 n.iter=1000000, n.burnin = 250000, n.thin = 250)
1022     mod.Z010.mcmc<-as.mcmc(mod.Z010)
1023     mZ010<-mod.Z010$BUGSoutput$sims.list
1024     mZ010.deviance<-mZ010$deviance
1025     mZ010.loglik<-mZ010$loglik
1026     dimSEM<-dim(mZ010.loglik)[1]
1027     list.mZ010<-sapply(1:dimSEM,function(x) matrix(mZ010.loglik[x,,],nrow=dim1*dim2))
1028     list.tmZ010<-(t(list.mZ010))
1029     mZ010.loo<-loo(list.tmZ010)
1030     mZ010.loo
1031     loo_file<-paste(dossier, "/", site, "_Z010_loo.txt", sep="")

```

```

1032     write_values("mZ010", app=T, loo_file)
1033     mZ010_loo_pointwise<-mZ010.loo$pointwise
1034     mZ010_loo_pareto_k<-mZ010.loo$pareto_k
1035     mZ010.loo$pareto_k<-NULL
1036     mZ010.loo$pointwise<-NULL
1037     write_values(as.matrix(mZ010.loo), app=T, loo_file)
1038     save.image(paste(dossier, "/", site, "_Z010.RData", sep=""))
1039 }
1040 ### MODEL Z09
1041 mZ09<-function(){
1042     init.funZ09 <-function(){
1043         list("tau_l" = rexp(1,10), "tau_P" = rexp(1,10), "beta" = rnorm(1,0,1), "delta" = rnorm(1,0,1),
1044 "theta0" = rnorm(1,0,1), "epsilon" = rnorm(1,0,1),
1045 "effet_l"=rnorm(dim1,0,1),"effet_P"=rnorm(dim2,0,1), "inter"=inter0)
1046     }
1047     mod.Z09<-jags(inits=init.funZ09,model.file = "modelZ09_code.txt",data =
1048 list("cooc","visit","ab_P","dim1","dim2"),parameters.to.save =
1049 c("mu","effet_l","effet_P","tau_l","tau_P","delta","beta","theta0","epsilon","loglik"),n.chains = 1,
1050 n.iter=1000000, n.burnin = 250000, n.thin = 250)
1051     mod.Z09.mcmc<-as.mcmc(mod.Z09)
1052     mZ09<-mod.Z09$BUGSoutput$sims.list
1053     mZ09.deviance<-mZ09$deviance
1054     mZ09.loglik<-mZ09$loglik
1055     dimSEM<-dim(mZ09.loglik)[1]
1056     list.mZ09<-sapply(1:dimSEM,function(x) matrix(mZ09.loglik[x,,],nrow=dim1*dim2))
1057     list.tmZ09<-(t(list.mZ09))

```

Code de champ modifié

Mis en forme : Anglais (Royaume-Uni)

```

1058     mZ09.loo<-loo(list.tmZ09)
1059     mZ09.loo
1060     loo_file<-paste(dossier, "/", site, "_Z09_loo.txt", sep="")
1061     write_values("mZ09", app=T, loo_file)
1062     mZ09_loo_pointwise<-mZ09.loo$pointwise
1063     mZ09_loo_pareto_k<-mZ09.loo$pareto_k
1064     mZ09.loo$pareto_k<-NULL
1065     mZ09.loo$pointwise<-NULL
1066     write_values(as.matrix(mZ09.loo), app=T, loo_file)
1067     save.image(paste(dossier, "/", site, "_Z09.RData", sep=""))
1068 }
1069 ### MODEL Z08
1070 mZ08<-function(){
1071     init.funZ08 <-function(){
1072         list("tau_I" = rexp(1,10), "tau_P" = rexp(1,10), "beta" = rnorm(1,0,1), "gamma" =
1073 rnorm(1,0,1), "theta0" = rnorm(1,0,1), "epsilon" = rnorm(1,0,1),
1074 "effet_I"=rnorm(dim1,0,1),"effet_P"=rnorm(dim2,0,1), "inter"=inter0)
1075     }
1076     mod.Z08<-jags(inits=init.funZ08,model.file = "modelZ08_code.txt",data =
1077 list("cooc","visit","ab_I","dim1","dim2"),parameters.to.save =
1078 c("mu","effet_I","effet_P","tau_I","tau_P","gamma","beta","theta0","epsilon","loglik"),n.chains = 1,
1079 n.iter=1000000, n.burnin = 250000, n.thin = 250)
1080     mod.Z08.mcmc<-as.mcmc(mod.Z08)
1081     mZ08<-mod.Z08$BUGSoutput$sims.list
1082     mZ08.deviance<-mZ08$deviance
1083     mZ08.loglik<-mZ08$loglik

```

```

1084     dimSEM<-dim(mZ08.loglik)[1]
1085     list.mZ08<-sapply(1:dimSEM,function(x) matrix(mZ08.loglik[x,,],nrow=dim1*dim2))
1086     list.tmZ08<-(t(list.mZ08))
1087     mZ08.loo<-loo(list.tmZ08)
1088     mZ08.loo
1089     loo_file<-paste(dossier, "/", site, "_Z08_loo.txt", sep="")
1090     write_values("mZ08", app=T, loo_file)
1091     mZ08_loo_pointwise<-mZ08.loo$pointwise
1092     mZ08_loo_pareto_k<-mZ08.loo$pareto_k
1093     mZ08.loo$pareto_k<-NULL
1094     mZ08.loo$pointwise<-NULL
1095     write_values(as.matrix(mZ08.loo), app=T, loo_file)
1096     save.image(paste(dossier, "/", site, "_Z08.RData", sep=""))
1097 }
1098 ### MODEL Z07
1099 mZ07<-function(){
1100     init.funZ07 <-function(){
1101         list("tau_I" = rexp(1,10), "tau_P" = rexp(1,10), "alpha" = 0.1,"beta" = rnorm(1,0,1), "delta" =
1102 rnorm(1,0,1), "theta0" = rnorm(1,0,1), "effet_I"=rnorm(dim1,0,1),"effet_P"=rnorm(dim2,0,1),
1103 "inter"=inter0)
1104     }
1105     mod.Z07<-jags(inits=init.funZ07,model.file = "modelZ07_code.txt",data =
1106 list("cooc","visit","ab_P","dim1","dim2"),parameters.to.save =
1107 c("mu","effet_I","effet_P","tau_I","tau_P","alpha","delta","beta","theta0","loglik"),n.chains = 1,
1108 n.iter=1000000, n.burnin = 250000, n.thin = 250)
1109     mod.Z07.mcmc<-as.mcmc(mod.Z07)

```

```

1110     mZ07<-mod.Z07$BUGSoutput$sims.list
1111     mZ07.deviance<-mZ07$deviance
1112     mZ07.loglik<-mZ07$loglik
1113     dimSEM<-dim(mZ07.loglik)[1]
1114     list.mZ07<-sapply(1:dimSEM,function(x) matrix(mZ07.loglik[x,,],nrow=dim1*dim2))
1115     list.tmZ07<-(t(list.mZ07))
1116     mZ07.loo<-loo(list.tmZ07)
1117     mZ07.loo
1118     loo_file<-paste(dossier, "/", site, "_Z07_loo.txt", sep="")
1119     write_values("mZ07", app=T, loo_file)
1120     mZ07_loo_pointwise<-mZ07.loo$pointwise
1121     mZ07_loo_pareto_k<-mZ07.loo$pareto_k
1122     mZ07.loo$pareto_k<-NULL
1123     mZ07.loo$pointwise<-NULL
1124     write_values(as.matrix(mZ07.loo), app=T, loo_file)
1125     save.image(paste(dossier, "/", site, "_Z07.RData", sep=""))
1126 }
1127 ### MODEL Z06
1128 mZ06<-function(){
1129     init.funZ06 <-function(){
1130         list("tau_I" = rexp(1,10), "tau_P" = rexp(1,10), "alpha" = 0.1,"beta" = rnorm(1,0,1), "gamma"
1131 = rnorm(1,0,1), "theta0" = rnorm(1,0,1), "effet_I"=rnorm(dim1,0,1),"effet_P"=rnorm(dim2,0,1),
1132 "inter"=inter0)
1133     }
1134     mod.Z06<-jags(inits=init.funZ06,model.file = "modelZ06_code.txt",data =
1135 list("cooc","visit","ab_I","dim1","dim2"),parameters.to.save =

```

Code de champ modifié

Mis en forme : Anglais (Royaume-Uni)


```

1136 c("mu","effet_l","effet_P","tau_l","tau_P","alpha","gamma","beta","theta0","loglik"),n.chains = 1,
1137 n.iter=1000000, n.burnin = 250000, n.thin = 250)
1138     mod.Z06.mcmc<-as.mcmc(mod.Z06)
1139     mZ06<-mod.Z06$BUGSoutput$sims.list
1140     mZ06.deviance<-mZ06$deviance
1141     mZ06.loglik<-mZ06$loglik
1142     dimSEM<-dim(mZ06.loglik)[1]
1143     list.mZ06<-sapply(1:dimSEM,function(x) matrix(mZ06.loglik[x,,],nrow=dim1*dim2))
1144     list.tmZ06<-t(list.mZ06)
1145     mZ06.loo<-loo(list.tmZ06)
1146     mZ06.loo
1147     loo_file<-paste(dossier, "/", site, "_Z06_loo.txt", sep="")
1148     write_values("mZ06", app=T, loo_file)
1149     mZ06_loo_pointwise<-mZ06.loo$pointwise
1150     mZ06_loo_pareto_k<-mZ06.loo$pareto_k
1151     mZ06.loo$pareto_k<-NULL
1152     mZ06.loo$pointwise<-NULL
1153     write_values(as.matrix(mZ06.loo), app=T, loo_file)
1154     save.image(paste(dossier, "/", site, "_Z06.RData", sep=""))
1155 }
1156 ### MODEL Z05
1157 mZ05<-function(){
1158     init.funZ05 <-function(){
1159         list("tau_l" = rexp(1,10), "tau_P" = rexp(1,10), "alpha" = 0.1,"beta" = rnorm(1,0,1), "theta0"
1160 = rnorm(1,0,1), "epsilon" = rnorm(1,0,1), "effet_l"=rnorm(dim1,0,1),"effet_P"=rnorm(dim2,0,1),
1161 "inter"=inter0)

```

Code de champ modifié

Mis en forme : Anglais (Royaume-Uni)

```

1162     }
1163     mod.Z05<-jags(inits=init.funZ05,model.file = "modelZ05_code.txt",data =
1164 list("coc","visit","dim1","dim2"),parameters.to.save =
1165 c("mu","effet_I","effet_P","tau_I","tau_P","alpha","beta","theta0","epsilon","loglik"),n.chains = 1,
1166 n.iter=1000000, n.burnin = 250000, n.thin = 250)
1167     mod.Z05.mcmc<-as.mcmc(mod.Z05)
1168     mZ05<-mod.Z05$BUGSoutput$sims.list
1169     mZ05.deviance<-mZ05$deviance
1170     mZ05.loglik<-mZ05$loglik
1171     dimSEM<-dim(mZ05.loglik)[1]
1172     list.mZ05<-sapply(1:dimSEM,function(x) matrix(mZ05.loglik[x,,],nrow=dim1*dim2))
1173     list.tmZ05<-(t(list.mZ05))
1174     mZ05.loo<-loo(list.tmZ05)
1175     mZ05.loo
1176     loo_file<-paste(dossier, "/", site, "_Z05_loo.txt", sep="")
1177     write_values("mZ05", app=T, loo_file)
1178     mZ05_loo_pointwise<-mZ05.loo$pointwise
1179     mZ05_loo_pareto_k<-mZ05.loo$pareto_k
1180     mZ05.loo$pareto_k<-NULL
1181     mZ05.loo$pointwise<-NULL
1182     write_values(as.matrix(mZ05.loo), app=T, loo_file)
1183     save.image(paste(dossier, "/", site, "_Z05.RData", sep=""))
1184 }
1185 ### MODEL Z04
1186 mZ04<-function(){
1187     init.funZ04 <-function(){
|

```

Code de champ modifié

Mis en forme : Anglais (Royaume-Uni)

```

1188     list("tau_I" = rexp(1,10), "tau_P" = rexp(1,10), "beta" = rnorm(1,0,1), "gamma" =
1189 rnorm(1,0,1), "delta" = rnorm(1,0,1), "theta0" = rnorm(1,0,1), "epsilon" = rnorm(1,0,1),
1190 "effet_I"=rnorm(dim1,0,1),"effet_P"=rnorm(dim2,0,1), "inter"=inter0)
1191     }
1192     mod.Z04<-jags(inits=init.funZ04,model.file = "modelZ04_code.txt",data =
1193 list("cooc","visit","ab_I","ab_P","dim1","dim2"),parameters.to.save =
1194 c("mu","effet_I","effet_P","tau_I","tau_P","gamma","delta","beta","theta0","epsilon","loglik"),n.chai
1195 ns = 1, n.iter=1000000, n.burnin = 250000, n.thin = 250)
1196     mod.Z04.mcmc<-as.mcmc(mod.Z04)
1197     mZ04<-mod.Z04$BUGSoutput$sims.list
1198     mZ04.deviance<-mZ04$deviance
1199     mZ04.loglik<-mZ04$loglik
1200     dimSEM<-dim(mZ04.loglik)[1]
1201     list.mZ04<-sapply(1:dimSEM,function(x) matrix(mZ04.loglik[x,,],nrow=dim1*dim2))
1202     list.tmZ04<-(t(list.mZ04))
1203     mZ04.loo<-loo(list.tmZ04)
1204     mZ04.loo
1205     loo_file<-paste(dossier, "/", site, "_Z04_loo.txt", sep="")
1206     write_values("mZ04", app=T, loo_file)
1207     mZ04_loo_pointwise<-mZ04.loo$pointwise
1208     mZ04_loo_pareto_k<-mZ04.loo$pareto_k
1209     mZ04.loo$pareto_k<-NULL
1210     mZ04.loo$pointwise<-NULL
1211     write_values(as.matrix(mZ04.loo), app=T, loo_file)
1212     save.image(paste(dossier, "/", site, "_Z04.RData", sep=""))
1213 }

```

```

1214 ### MODEL Z03
1215 mZ03<-function(){
1216     init.funZ03 <-function(){
1217         list("tau_I" = rexp(1,10), "tau_P" = rexp(1,10), "alpha" = 0.1,"beta" = rnorm(1,0,1), "gamma"
1218 = rnorm(1,0,1), "theta0" = rnorm(1,0,1), "epsilon" = rnorm(1,0,1),
1219 "effet_I"=rnorm(dim1,0,1),"effet_P"=rnorm(dim2,0,1), "inter"=inter0)
1220     }
1221     mod.Z03<-jags(inits=init.funZ03,model.file = "modelZ03_code.txt",data =
1222 list("cooc","visit","ab_I","dim1","dim2"),parameters.to.save =
1223 c("mu","effet_I","effet_P","tau_I","tau_P","alpha","gamma","beta","theta0","epsilon","loglik"),n.cha
1224 ins = 1, n.iter=1000000, n.burnin = 250000, n.thin = 250)
1225     mod.Z03.mcmc<-as.mcmc(mod.Z03)
1226     mZ03<-mod.Z03$BUGSoutput$sims.list
1227     mZ03.deviance<-mZ03$deviance
1228     mZ03.loglik<-mZ03$loglik
1229     dimSEM<-dim(mZ03.loglik)[1]
1230     list.mZ03<-sapply(1:dimSEM,function(x) matrix(mZ03.loglik[x,,],nrow=dim1*dim2))
1231     list.tmZ03<-(t(list.mZ03))
1232     mZ03.loo<-loo(list.tmZ03)
1233     mZ03.loo
1234     loo_file<-paste(dossier, "/", site, "_Z03_loo.txt", sep="")
1235     write_values("mZ03", app=T, loo_file)
1236     mZ03_loo_pointwise<-mZ03.loo$pointwise
1237     mZ03_loo_pareto_k<-mZ03.loo$pareto_k
1238     mZ03.loo$pareto_k<-NULL
1239     mZ03.loo$pointwise<-NULL

```

```

1240     write_values(as.matrix(mZ03.loo), app=T, loo_file)
1241     save.image(paste(dossier, "/", site, "_Z03.RData", sep=""))
1242 }
1243 ### MODEL Z02
1244 mZ02<-function(){
1245     init.funZ02 <-function(){
1246         list("tau_I" = rexp(1,10), "tau_P" = rexp(1,10), "alpha" = 0.1, "beta" = rnorm(1,0,1), "delta" =
1247 rnorm(1,0,1), "theta0" = rnorm(1,0,1), "epsilon" = rnorm(1,0,1),
1248 "effet_I"=rnorm(dim1,0,1),"effet_P"=rnorm(dim2,0,1), "inter"=inter0)
1249     }
1250     mod.Z02<<-jags(inits=init.funZ02,model.file = "modelZ02_code.txt",data =
1251 list("cooc","visit","ab_P","dim1","dim2"),parameters.to.save =
1252 c("mu","effet_I","effet_P","tau_I","tau_P","alpha","delta","beta","theta0","epsilon","loglik"),n.chain
1253 s = 1, n.iter=1000000, n.burnin = 250000, n.thin = 250)
1254     mod.Z02.mcmc<-as.mcmc(mod.Z02)
1255     mZ02<-mod.Z02$BUGSoutput$sims.list
1256     mZ02.deviance<-mZ02$deviance
1257     mZ02.loglik<-mZ02$loglik
1258     dimSEM<-dim(mZ02.loglik)[1]
1259     list.mZ02<-sapply(1:dimSEM,function(x) matrix(mZ02.loglik[x,,],nrow=dim1*dim2))
1260     list.tmZ02<-(t(list.mZ02))
1261     mZ02.loo<-loo(list.tmZ02)
1262     mZ02.loo
1263     loo_file<-paste(dossier, "/", site, "_Z02_loo.txt", sep="")
1264     write_values("mZ02", app=T, loo_file)
1265     mZ02_loo_pointwise<-mZ02.loo$pointwise

```

```

1266     mZ02_loo_pareto_k<-mZ02.loo$pareto_k
1267     mZ02.loo$pareto_k<-NULL
1268     mZ02.loo$pointwise<-NULL
1269     write_values(as.matrix(mZ02.loo), app=T, loo_file)
1270     save.image(paste(dossier, "/", site, "_Z02.RData", sep=""))
1271 }
1272 ### MODEL Z01
1273 mZ01<-function(){
1274     init.funZ01 <-function(){
1275         list("tau_I" = rexp(1,10), "tau_P" = rexp(1,10), "alpha" = 0.1,"beta" = rnorm(1,0,1), "gamma"
1276 = rnorm(1,0,1), "delta" = rnorm(1,0,1), "theta0" = rnorm(1,0,1),
1277 "effet_I"=rnorm(dim1,0,1),"effet_P"=rnorm(dim2,0,1), "inter"=inter0)
1278     }
1279     mod.Z01<-jags(inits=init.funZ01,model.file = "modelZ01_code.txt",data =
1280 list("cooc","visit","ab_I","ab_P", "dim1", "dim2"),parameters.to.save =
1281 c("mu","effet_I","effet_P","tau_I","tau_P","alpha","gamma","delta","beta","theta0","loglik"),n.chain
1282 s = 1, n.iter=1000000, n.burnin = 250000, n.thin = 250)
1283     mod.Z01.mcmc<-as.mcmc(mod.Z01)
1284     mZ01<-mod.Z01$BUGSoutput$sims.list
1285     mZ01.deviance<-mZ01$deviance
1286     mZ01.loglik<-mZ01$loglik
1287     dimSEM<-dim(mZ01.loglik)[1]
1288     list.mZ01<-sapply(1:dimSEM,function(x) matrix(mZ01.loglik[x,,],nrow=dim1*dim2))
1289     list.tmZ01<-(t(list.mZ01))
1290     mZ01.loo<-loo(list.tmZ01)
1291     mZ01.loo

```

```

1292     loo_file<-paste(dossier, "/", site, "_Z01_loo.txt", sep="")
1293     write_values("mZ01", app=T, loo_file)
1294     mZ01_loo_pointwise<-mZ01.loo$pointwise
1295     mZ01_loo_pareto_k<-mZ01.loo$pareto_k
1296     mZ01.loo$pareto_k<-NULL
1297     mZ01.loo$pointwise<-NULL
1298     write_values(as.matrix(mZ01.loo), app=T, loo_file)
1299     save.image(paste(dossier, "/", site, "_Z01.RData", sep=""))
1300 }
1301 ### MODEL Z00
1302 mZ00<-function(){
1303     init.funZ00 <-function(){
1304         list("tau_I" = rexp(1,10), "tau_P" = rexp(1,10), "alpha" = 0.1,"beta" = rnorm(1,0,1), "gamma"
1305 = rnorm(1,0,1), "delta" = rnorm(1,0,1), "theta0" = rnorm(1,0,1), "epsilon" = rnorm(1,0,1),
1306 "effet_I"=rnorm(dim1,0,1),"effet_P"=rnorm(dim2,0,1), "inter"=inter0)
1307     }
1308     mod.Z00<-jags(inits=init.funZ00,model.file = "modelZ00_code.txt",data =
1309 list("cooc","visit","ab_I","ab_P","dim1","dim2"),parameters.to.save =
1310 c("mu","effet_I","effet_P","tau_I","tau_P","alpha","gamma","delta","beta","theta0","epsilon","loglik
1311 "),n.chains = 1, n.iter=1000000, n.burnin = 250000, n.thin = 250)
1312     mod.Z00.mcmc<-as.mcmc(mod.Z00)
1313     mZ00<-mod.Z00$BUGSoutput$sims.list
1314     mZ00.deviance<-mZ00$deviance
1315     mZ00.loglik<-mZ00$loglik
1316     dimSEM<-dim(mZ00.loglik)[1]
1317     list.mZ00<-sapply(1:dimSEM,function(x) matrix(mZ00.loglik[x,,],nrow=dim1*dim2))

```

```

1318     list.tmZ00<-t(list.mZ00)
1319     mZ00.loo<-loo(list.tmZ00)
1320     mZ00.loo
1321     loo_file<-paste(dossier, "/", site, "_Z00_loo.txt", sep="")
1322     write_values("mZ00", app=T, loo_file)
1323     mZ00_loo_pointwise<-mZ00.loo$pointwise
1324     mZ00_loo_pareto_k<-mZ00.loo$pareto_k
1325     mZ00.loo$pareto_k<-NULL
1326     mZ00.loo$pointwise<-NULL
1327     write_values(as.matrix(mZ00.loo), app=T, loo_file)
1328     save.image(paste(dossier, "/", site, "_Z00.RData", sep=""))
1329 }
1330 ##### end model functions
1331 print("JOB DONE")
1332 #####
1333 ###   Network information (do not change)   ###
1334 #####
1335 #####BLOCK 3 – MODEL EXECUTION #####
1336 #launch_modele<-function(){
1337     ntw<-read.table(paste(dossier, "/", site, "_ntw.txt", sep=""),
1338 sep="\t",header=T,row.names=1)
1339     dim1<-dim(ntw)[1]
1340     dim2<-dim(ntw)[2]
1341     web<-as.matrix(ntw,dim1,dim2)
1342     inter0<-dget(paste(dossier, "/", site, "_web_i.txt", sep=""))
1343     cooc<-dget(paste(dossier, "/", site, "_co.txt", sep=""))

```

Code de champ modifié

Mis en forme : Anglais (Royaume-Uni)


```

1344 visit<-read.table(paste(dossier, "/", site, "_ntw.txt", sep=""),sep="\t",header=T)
1345 visit<-as.matrix(visit)
1346 abundancel<-read.table(paste(dossier, "/", site, "_abl.txt", sep=""), sep="\t", header=T)
1347 ab_I <- log(abundancel[,2])
1348 abundanceP<-read.table(paste(dossier, "/", site, "_abP.txt", sep=""), sep="\t", header=T)
1349 ab_P <- log(abundanceP[,2])
1350 if(opt$modele == "all")
1351 {
1352     print("modele: all")
1353     for(i in 0:15)
1354     {
1355         print(paste("COMPUTING MODELE ", i, "\n", sep=""))
1356         mod<-eval(parse(text=paste("mZ0", i, sep="")))
1357         mod()
1358     }
1359 }
1360 }else{
1361     print(paste("modele: ", opt$modele), sep="")
1362     mod<-eval(parse(text=paste("m", opt$modele, sep=""))) #recupération de la
1363 fonction du modele
1364     mod()
1365 }
1366 ##### end model execution
1367 #launch_modele()
1368
1369 #####PARAMETER VALUES#####

```

Code de champ modifié

Mis en forme : Anglais (Royaume-Uni)

```

1370 library(optparse)
1371 option_list = list(
1372     make_option(c("-d", "--dir"), type="character", default=NULL, help="model directory",
1373     metavar="character"),
1374     make_option(c("-s", "--site"), type="character", default=NULL, help="site name",
1375     metavar="character"))
1376 opt_parser = OptionParser(option_list=option_list);
1377 opt = parse_args(opt_parser);
1378 rdata<-list.files(opt$dir, pattern="*_Z015.RData")
1379 load(paste(opt$dir, "/", rdata, sep="")) #chargement du RData qui contient tous les modèles pour un
1380 site donné
1381 print(paste("RData ", rdata, " loaded", sep=""))
1382 for(mod in ls(pattern="mod.Z0*"))
1383 {
1384     print(paste("getting values from ", mod, sep=""))
1385     model<-eval(parse(text=mod))
1386     if(is.null(model$BUGSoutput$mean$alpha)){model$BUGSoutput$mean$alpha<-NA}
1387     if(is.null(model$BUGSoutput$mean$beta)){model$BUGSoutput$mean$beta<-NA}
1388     if(is.null(model$BUGSoutput$mean$delta)){model$BUGSoutput$mean$delta<-NA}
1389     if(is.null(model$BUGSoutput$mean$epsilon)){model$BUGSoutput$mean$epsilon<-NA}
1390     if(is.null(model$BUGSoutput$mean$gamma)){model$BUGSoutput$mean$gamma<-NA}
1391     val<-matrix(c(model$BUGSoutput$mean$alpha, model$BUGSoutput$mean$beta,
1392     model$BUGSoutput$mean$delta, model$BUGSoutput$mean$epsilon,
1393     model$BUGSoutput$mean$gamma), 1, 5, dimnames=list("values", c("alpha", "beta", "delta",
1394     "epsilon", "gamma")))

```

```
1395     write.table(val, file=paste(opt$dir, "/", opt$site, "_", mod, "_values.txt", sep=""), quote=F,  
1396     sep="\t", row.names=F, col.names=T)  
1397 }  
1398
```

Code de champ modifié

Mis en forme : Anglais (Royaume-Uni)

1399 **Appendix S3: Modularity and latent block model analysis**

1400 We calculated the modularity of the network using the `cluster_leading_eigen` method for
1401 modularity optimization implemented in the `igraph` package (Csardi and Nepusz 2006, Newman
1402 2006). We then performed latent block models (LBM) using the `BM_poisson` method for
1403 quantitative network data implemented in the `blockmodels` package (Leger et al. 2015). Blocks
1404 are calculated separately for the two groups (insect and plant) based on the number of visits (*i.e.* a
1405 weighted network). The algorithm finds the best divisions of insects and plants through fitting one
1406 Poisson parameter in each block of the visit matrix, thus essentially maximizing the ICL (Integrated
1407 Completed Likelihood; Biernacki et al. 2000, Daudin et al. 2007).

```
1408  
1409 library(bipartite)  
1410 library(vegan)  
1411 library(igraph)  
1412 library(dummies)  
1413 library(blockmodels)  
1414 library(ade4)  
1415 library(fields)  
1416  
1417 #site data (ex: Bois de Fontaret, BFs)  
1418 BFs<-read.table("ntwBFs.txt",header=T,sep="\t")  
1419 webBFs <- as.matrix(BFs)  
1420 ##### Modularity analysis, binary data #####  
1421 BFs.graph.bin<-graph_from_incidence_matrix(webBFs,multiple=F) #binary  
1422 BFs.bin.cle<-cluster_leading_eigen(BFs.graph.bin)  
1423 BFs.bin.cle  
1424 #get phenology overlap matrix
```

Code de champ modifié
Mis en forme : Anglais (Royaume-Uni)

```

1425 coBF<-dget("coBFs.txt")
1426 ##### LBM code: LBM analysis following Poisson #####
1427 bmi_BFs<-BM_poisson('LBM', webBFs)
1428 bmi_BFs$estimate()
1429 numi_BFs<-which.max(bmi_BFs$ICL)
1430 densi_BFs<-sum(webBFs)/(nrow(webBFs)*ncol(webBFs))
1431 probi_BFs<-bmi_BFs$model_parameters[[numi_BFs]]$lambda
1432 row.nb.gpi<-nrow(probi_BFs)
1433 col.nb.gpi<-ncol(probi_BFs)
1434 prob.rowi<-bmi_BFs$memberships[[numi_BFs]]$Z1
1435 hh.namei<-rownames(webBFs)
1436 mbrshp.hhi<-apply(prob.rowi,1,which.max)
1437 ls.freq.rowi<-rowSums(webBFs)
1438 res.hhi<-cbind.data.frame(hh.namei=hh.namei, mbrshp.hhi=mbrshp.hhi, freq.hhi=ls.freq.rowi)
1439 res.hh.ordi<-res.hhi[order(res.hhi$freq.hhi),]
1440 cpt=0
1441 for(k in 1: (nrow(res.hh.ordi)-1))
1442 {
1443   if (res.hh.ordi$mbrshp.hhi[k] !=res.hh.ordi$mbrshp.hhi[k+1]) cpt=cpt+1
1444 }
1445 nb.diff.hhi=cpt-(length(levels(as.factor(res.hh.ordi$mbrshp.hhi)))-1)
1446 #write tables
1447 write.table(res.hh.ordi,sep="\t",row.names=FALSE)
1448 prob.coli<-bmi_BFs$memberships[[numi_BFs]]$Z2
1449 sp.namei<-colnames(webBFs)
1450 mbrshp.spi<-apply(prob.coli,1,which.max)

```

Code de champ modifié

Mis en forme : Anglais (Royaume-Uni)

```

1451 ls.freq.coli<-colSums(webBFs)
1452 res.spi<-cbind.data.frame(sp.namei=sp.namei, mbrshp.spi=mbrshp.spi, freq.spi=ls.freq.coli)
1453 res.sp.ordi<-res.spi[order(res.spi$freq.spi),]
1454 cpt=0
1455 for (k in 1: (nrow(res.sp.ordi)-1))
1456 {
1457   if(res.sp.ordi$mbrshp.spi[k] !=res.sp.ordi$mbrshp.spi[k+1]) cpt=cpt+1
1458 }
1459 nb.diff.spi=cpt-(length(levels(as.factor(res.sp.ordi$mbrshp.spi)))-1)
1460 res.sp.ord2i=res.spi[order(res.spi$mbrshp.spi),]
1461 write.table(res.sp.ordi,sep="\t",row.names=FALSE)
1462 write.table(probi_BFs,file="_prob_BFs",sep="\t",row.names=FALSE)
1463
1464 ##### Matrix organization #####
1465 par(mfrow=c(1,1))
1466 webBFs2<-webBFs
1467 webBFs[which(webBFs>1)]=1
1468 nb.row=nrow(webBFs)
1469 nb.col=ncol(webBFs)
1470 nds=webBFs
1471 nps=coBF
1472 res.prob=read.table("_prob_BFs",sep="\t",h=TRUE)
1473 ls.ord.col.prob=order(colSums(res.prob),decreasing=TRUE)
1474 ls.ord.row.prob=order(rowSums(res.prob),decreasing=TRUE)
1475 ls.ord.hhi=sapply(res.hhi$mbrshp.hhi,function(x) which (x==ls.ord.row.prob))
1476 res.hh.ord2i=res.hhi[order(ls.ord.hhi),]

```

```

1477 row.nb.gpi=length(levels(as.factor(res.hhi$mbrshp.hhi)))
1478 res.hh.ord3i=NULL
1479 for (h in ls.ord.row.prob)
1480 {
1481   part=res.hh.ord2i[res.hh.ord2i$mbrshp.hhi==h,]
1482   part.ord=part[order(part$freq.hhi,decreasing=TRUE),]
1483   res.hh.ord3i=rbind.data.frame(res.hh.ord3i,part.ord)
1484 }
1485 ls.ord.sp=sapply(res.spi$mbrshp.spi,function(x) which (x==ls.ord.col.prob))
1486 res.sp.ord2i=res.spi[order(ls.ord.sp),]
1487 col.nb.gb=length(levels(as.factor(res.spi$mbrshp.spi)))
1488 res.sp.ord3i=NULL
1489 for (h in ls.ord.col.prob)
1490 {
1491   part=res.sp.ord2i[res.sp.ord2i$mbrshp.spi==h,]
1492   part.ord=part[order(part$freq.spi,decreasing=TRUE),]
1493   res.sp.ord3i=rbind.data.frame(res.sp.ord3i,part.ord)
1494 }
1495 nds=nds[as.character(res.hh.ord3i$hh.namei),as.character(res.sp.ord3i$sp.namei)]
1496 nps=nps[as.character(res.hh.ord3i$hh.namei),as.character(res.sp.ord3i$sp.namei)]
1497 webBFs2=webBFs2[as.character(res.hh.ord3i$hh.namei),as.character(res.sp.ord3i$sp.namei)]
1498
1499 ##### Plot matrix with heatcolours and the number of visits #####
1500 visits<-matrix(webBFs2,nrow=dim(webBFs2)[1]*dim(webBFs2)[2],ncol=1)
1501 visits<-visits[which(visits>0)] #without the zeros
1502 coord.function<-function(x,nI,nP){

```

Code de champ modifié

Mis en forme : Anglais (Royaume-Uni)

```

1503   c(((x-1)%%nl)+1,((x-1)%/%nl)+1)
1504 }
1505 func.plot.matrix<-function(x,y){
1506   indices<-which(x==1)
1507   min<-min(y)
1508   max<-max(y)
1509   yLabels<-rownames(x)
1510   xLabels<-colnames(x)
1511   title<-c("Bois de Fontaret")
1512   if(is.null(xLabels)){
1513     xLabels<-c(1:ncol(x))
1514   }
1515   if(is.null(yLabels)){
1516     yLabels<-c(1:nrow(x))
1517   }
1518   reverse<-nrow(x):1
1519   yLabels<-yLabels[reverse]
1520   y<-y[reverse,]
1521   image.plot(1:length(xLabels),1:length(yLabels),t(y),col=c("white",heat.colors(12)[12:1]), xlab="",
1522   ylab="",axes=FALSE,zlim=c(min,max))
1523   if(!is.null(title)){
1524     title(ylab="Insects", line=8, cex.lab=1)
1525     title(xlab="Plants", line=6, cex.lab=1.2)
1526     title("Bois de Fontaret")
1527   }
1528   axis(BELOW<-1,at=1:length(xLabels),labels=as.factor(as.character(xLabels)),las =2, cex.axis=0.6)

```

Code de champ modifié

Mis en forme : Anglais (Royaume-Uni)

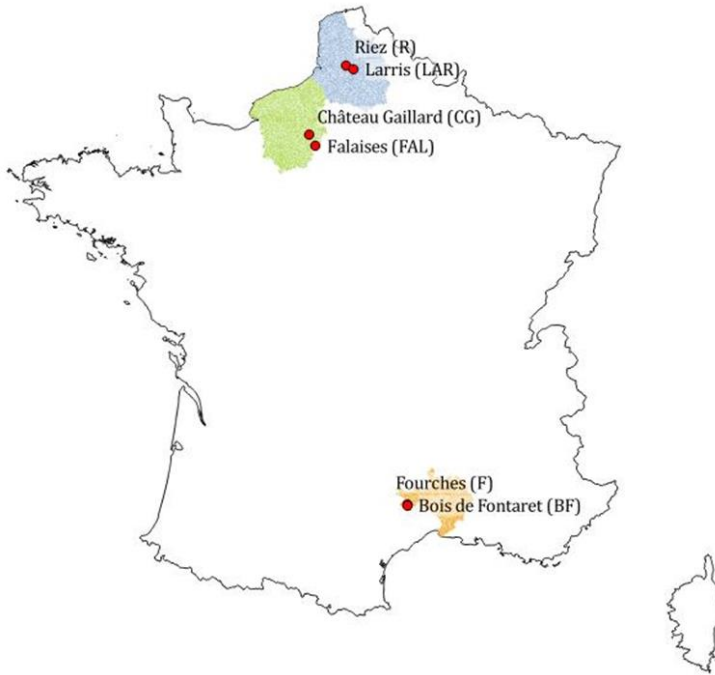

```

1529 axis(LEFT<-2,at=1:length(yLabels), labels=as.factor(as.character(yLabels)),las= 2,cex.axis=0.6)
1530 axis(BELOW<-1,at=1:length(xLabels),labels=rep("",length(xLabels)),las =2,cex.axis=0.6)
1531 axis(LEFT<-2,at=1:length(yLabels),labels=rep("",length(yLabels)),las=2,cex.axis<-0.6)
1532 coo<-t(rbind(sapply(indices,function(xx) coord.function(xx,nrow(x),ncol(x)))))
1533 text(coo[,2],nrow(webBFs)+1-coo[,1],labels=visits, cex=0.6)
1534 }
1535 func.plot.matrix(nds,nps)
1536 ##### Black lines to delimit blocks in the plot #####
1537 if (row.nb.gpi>1)
1538 {
1539   ls.class=as.numeric(as.data.frame(table(res.hh.ord2i$mbrshp.hhi))[ls.ord.row.prob,2])
1540   ls.cum=sum(ls.class)-cumsum(ls.class)
1541   abline(h=ls.cum+0.5,col="grey20", lwd=3)
1542 }
1543 if (col.nb.gpi>1)
1544 {
1545   ls.class=as.numeric(as.data.frame(table(res.sp.ord2i$mbrshp.spi))[ls.ord.col.prob,2])
1546   ls.cum=cumsum(ls.class)
1547   abline(v=ls.cum+0.5,col="grey20", lwd=3)
1548 }

```

1549

Figures and Tables



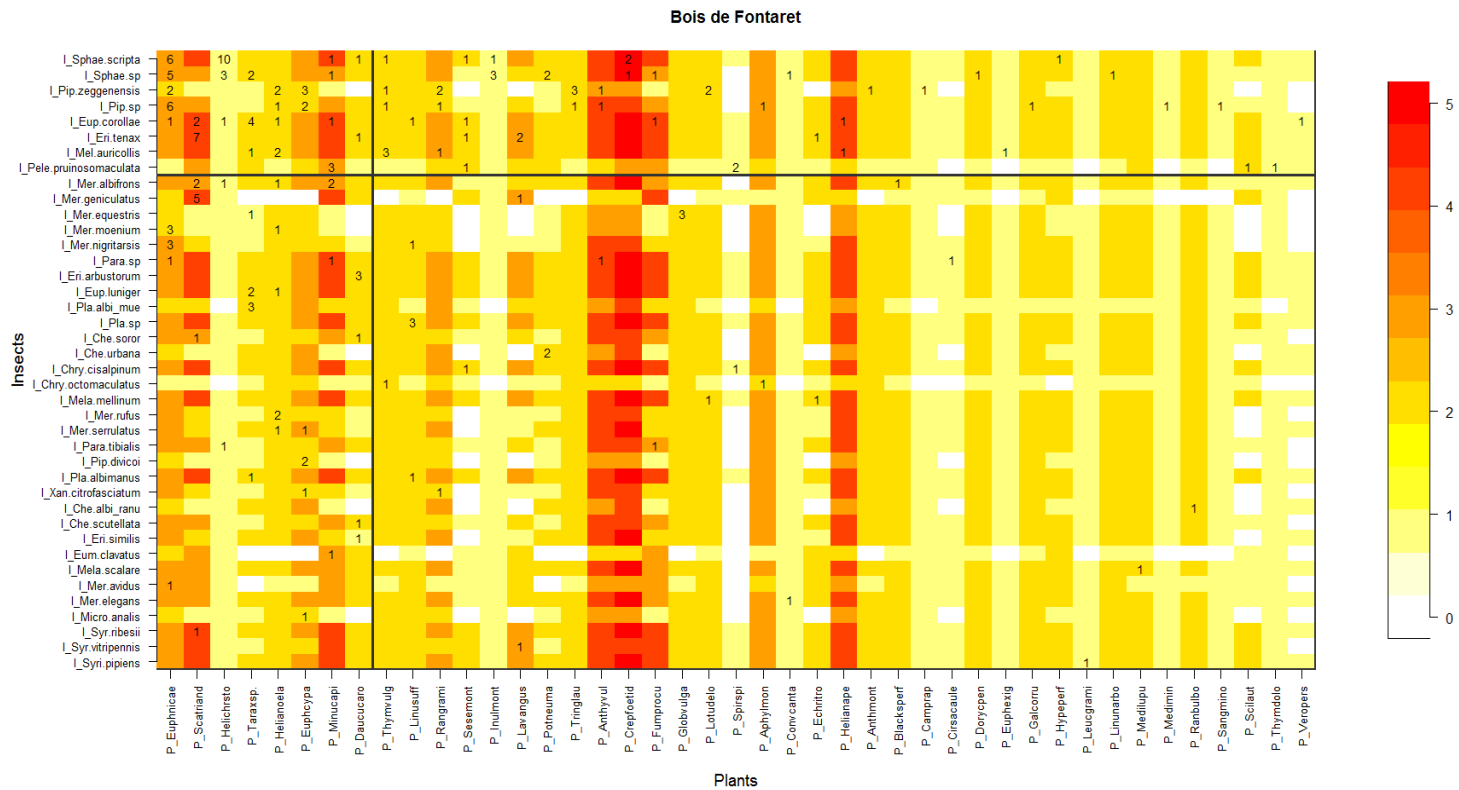
1550

1551 Figure S1. Site location in France: in blue the French départements Pas-de-Calais and Somme (Hauts-
1552 de-France region), in green the départements Eure and Seine Maritime (Normandie region), in orange
1553 the département Gard (Occitanie region). The six sites correspond to the red dots.

1554

Code de champ modifié

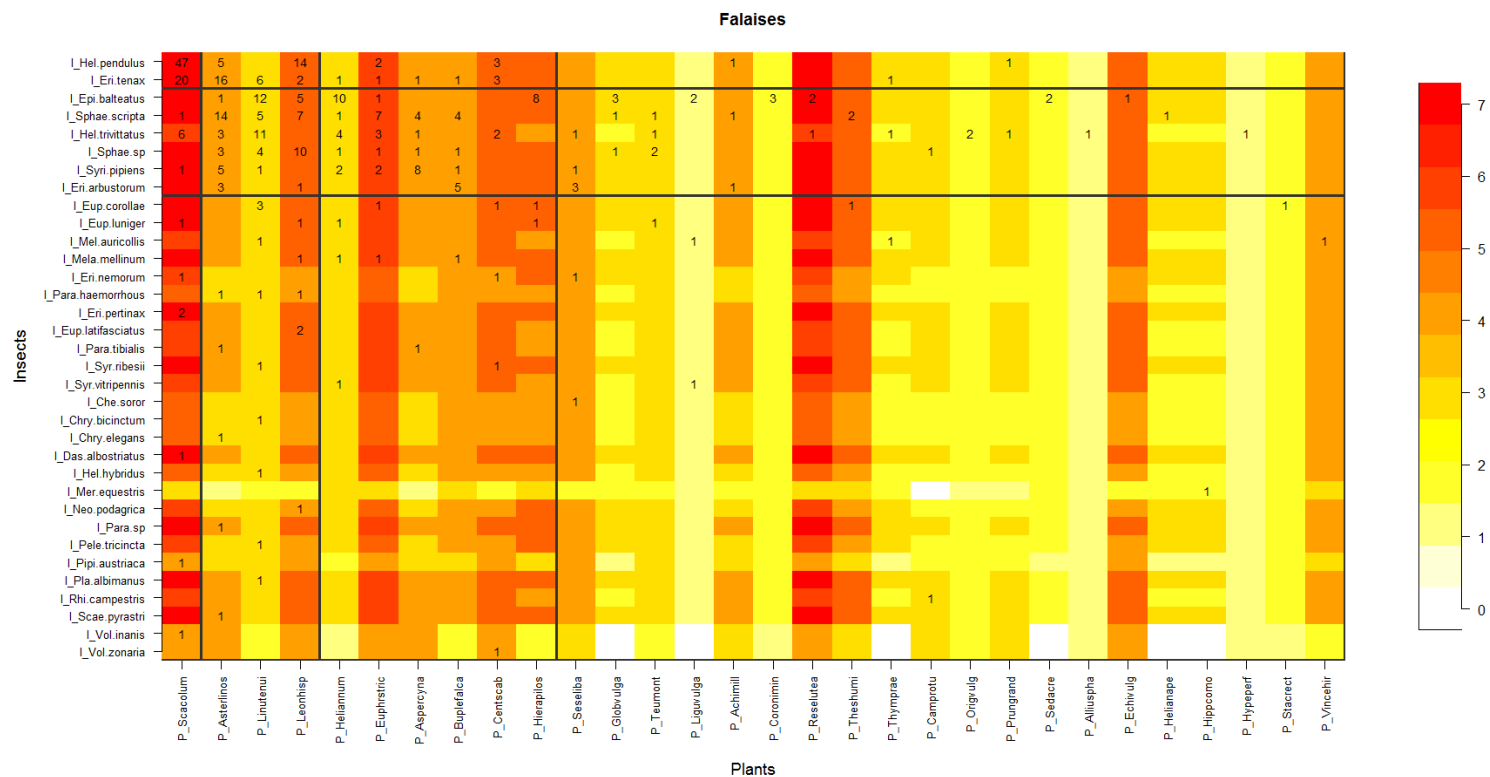
Mis en forme : Anglais (Royaume-Uni)



1555

1556 Figure S2. Block clustering provided by LBM in the site of Bois de Fontaret (BF, Occitanie), overlaid on a heatmap of species phenology overlap. Insect species
 1557 are displayed in rows and plant species in columns, following their degree (number of partners). The blocks of insects and the blocks of plants are separated
 1558 by solid black lines. Colours correspond to the number of months that are shared by each pair of plant and insect species (PO, phenology overlap), with higher
 1559 PO corresponding to darker colours. Numbers are the number of visits observed in the field for a given plant-insect pair.

Code de champ modifié
 Mis en forme : Anglais (Royaume-Uni)

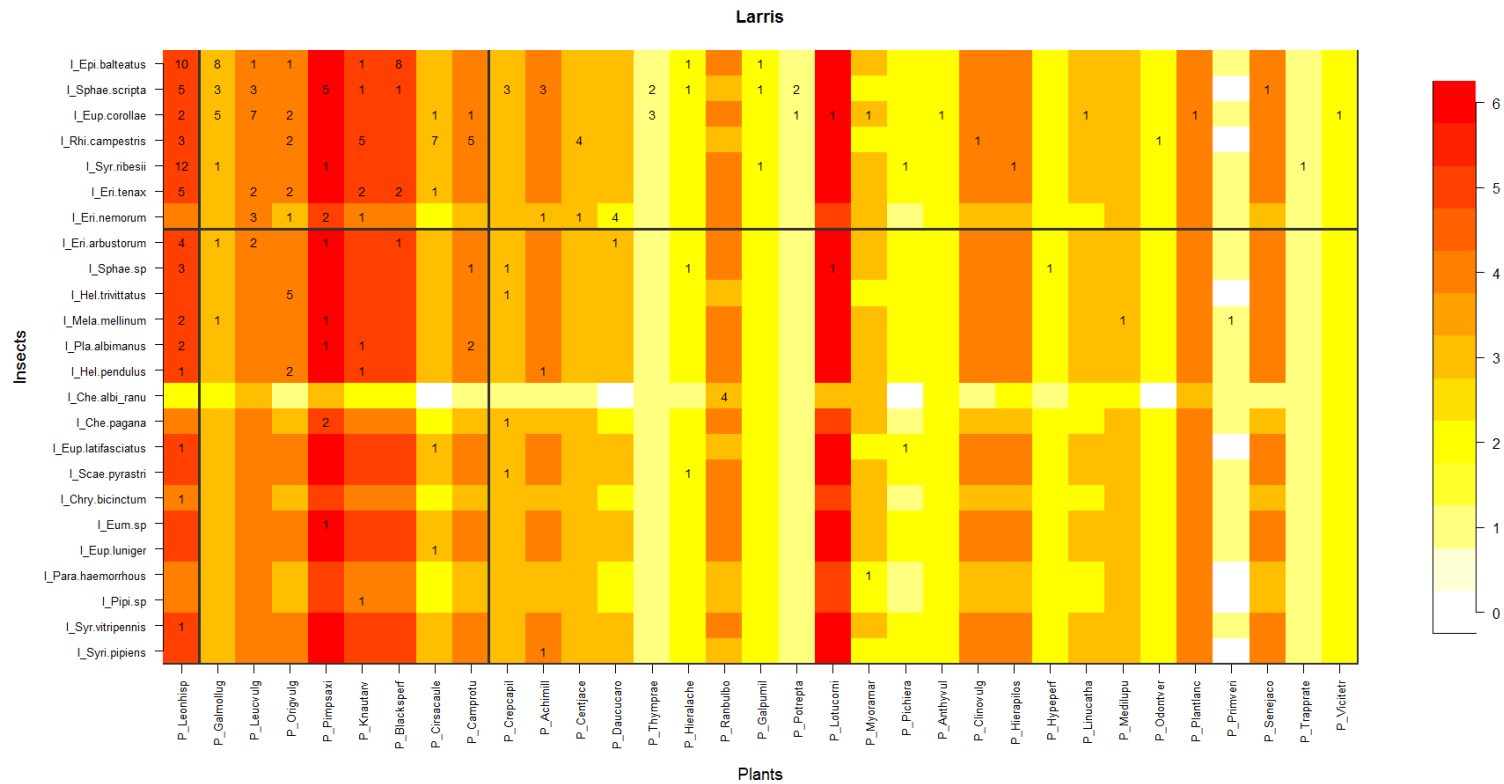


1560

1561 Figure S3. Block clustering provided by LBM in the site of Falaises (FAL, Normandie), overlaid on a heatmap of species phenology overlap. Insect species are
 1562 displayed in rows and plant species in columns, following their degree (number of partners). The blocks of insects and the blocks of plants are separated by
 1563 solid black lines. Colours correspond to the number of months that are shared by each pair of plant and insect species (PO, phenology overlap), with higher
 1564 PO corresponding to darker colours. Numbers are the number of visits observed in the field for a given plant-insect pair.

Code de champ modifié

Mis en forme : Anglais (Royaume-Uni)

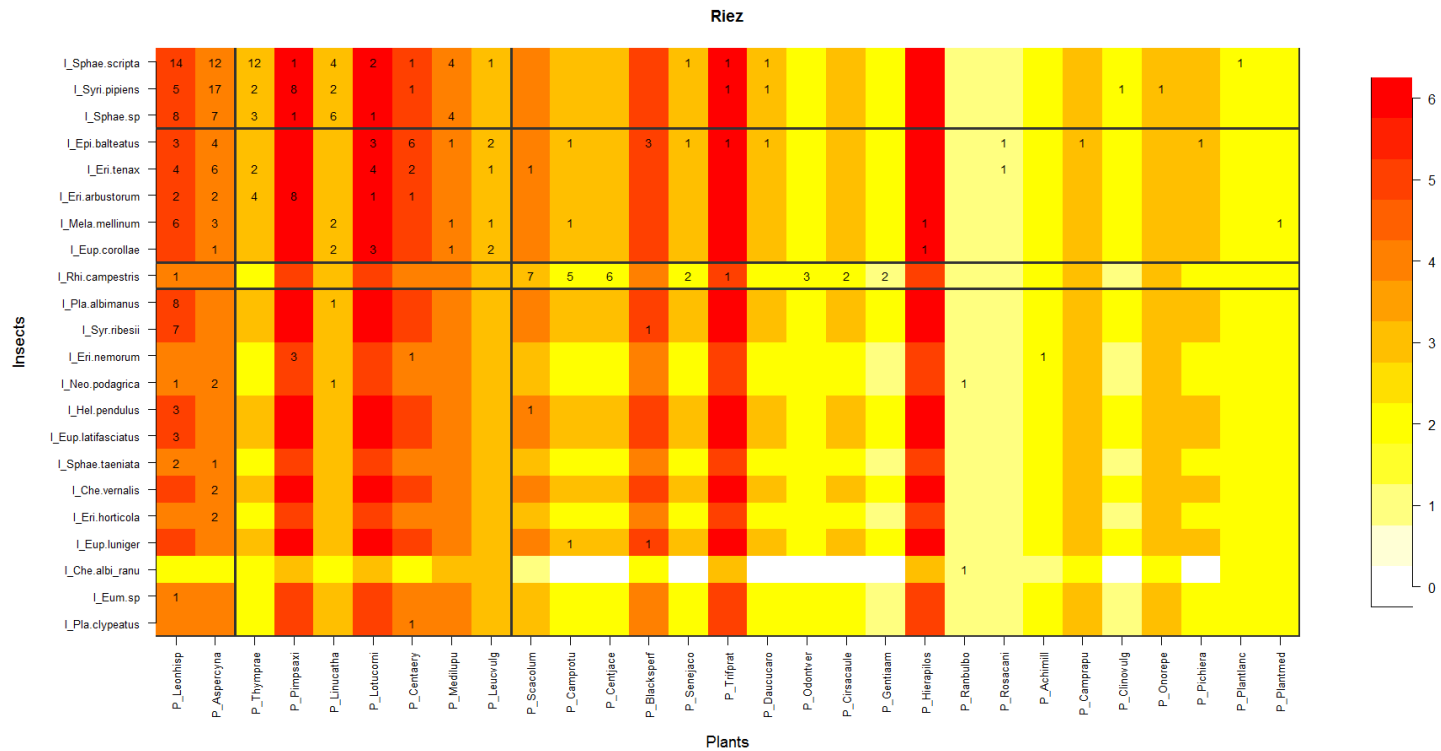


1565

1566 Figure S4. Block clustering provided by LBM in the site of Larris (LAR, Hauts-de-France), overlaid on a heatmap of species phenology overlap. Insect species
 1567 are displayed in rows and plant species in columns, following their degree (number of partners). The blocks of insects and the blocks of plants are separated
 1568 by solid black lines. Colours correspond to the number of months that are shared by each pair of plant and insect species (PO, phenology overlap), with higher
 1569 PO corresponding to darker colours. Numbers are the number of visits observed in the field for a given plant-insect pair.

Code de champ modifié

Mis en forme : Anglais (Royaume-Uni)



1570

1571 Figure S5. Block clustering provided by LBM in the site of Riez (R, Hauts-de-France), overlaid on a heatmap of species phenology overlap. Insect species are
 1572 displayed in rows and plant species in columns, following their degree (number of partners). The blocks of insects and the blocks of plants are separated by
 1573 solid black lines. Colours correspond to the number of months that are shared by each pair of plant and insect species (PO, phenology overlap), with higher
 1574 PO corresponding to darker colours. Numbers are the number of visits observed in the field for a given plant-insect pair.

Code de champ modifié

Mis en forme : Anglais (Royaume-Uni)

1575 Table S1. Table of transformed plant abundances. The first column shows the Braun-Blanquet
1576 coefficients of, the second column, their percentages, and the third column, the transformed
1577 abundances used as the plant abundances in the model.

Coefficient Braun-Blanquet	Abundance percentage interval	Abundance percentage
<i>i</i>	1 individual	0.1%
<i>+</i>	< 1 %	0.5%
<i>1</i>	1-10 %	5%
<i>2</i>	10-25 %	15%
<i>3</i>	25-50 %	35%
<i>4</i>	50-75 %	65%
<i>5</i>	75-100 %	85%

1578

